EFFECTS OF MASS WASTING AND UPLIFT ON FLUVIAL NETWORKS WITHIN THE CENTRAL FRANCISCAN MÉLANGE COMPLEX – EEL RIVER, CA

by

SAMUEL W. SHAW

A THESIS

Presented to the Department of Earth Sciences
and the Graduate School of the University of Oregon
in partial fulfillment of the requirements
for the degree of
Master of Science

September 2017

THESIS APPROVAL PAGE

Student: Samuel W. Shaw

Title: Effects of Mass Wasting and Uplift on Fluvial Networks within the Franciscan Mélange Complex – Eel River, CA

This thesis has been accepted and approved in partial fulfillment of the requirements for the Master of Science degree in the Department of Earth Sciences by:

Joshua Roering	Chairperson
Alan Rempel	Member
Leif Karlstrom	Member

and

Sara D. Hodges	Interim Vice Provost and Dean of the Graduate School

Original approval signatures are on file with the University of Oregon Graduate School.

Degree awarded September 2017

THESIS ABSTRACT

Samuel W. Shaw

Master of Science

Department of Earth Sciences

September 2017

Title: Effects of Mass Wasting and Uplift on Fluvial Networks within the Franciscan Mélange Complex – Eel River, CA

The Eel River watershed has a high concentration of slow-moving landslides, or earthflows, due to argillaceous mélange bedrock and high tectonic uplift. Earthflows within this area are highly dissected by ephemeral channels, or gullies. Despite the pervasiveness of gullying in this area, the role of fluvial systems in relation to earthflows and varying uplift is poorly understood. To understand the role of earthflows and tectonics in dictating channel processes, we investigate channels in areas of differential uplift and mass failure activity.

Channel networks are connected and continuous in catchments without earthflows, and disconnected and prone to bank failure on earthflow surfaces. Gully profiles are influenced BY earthflow undulations, which attenuate with fluvial incision after earthflows cease activity. We find notable differences in fluvial dissection between areas of high and low landslide activity. We find that mass wasting and local bedrock have a strong influence on formation and organization of channels.

CURRICULUM VITAE

NAME OF AUTHOR: Samuel W. Shaw

GRADUATE AND UNDERGRADUATE SCHOOLS ATTENDED:

University of Oregon, Eugene
University of Pennsylvania, Philadelphia

DEGREES AWARDED:

Master of Science, Earth Sciences, 2017, University of Oregon
Bachelor of Arts, Geology, 2014, University of Pennsylvania

AREAS OF SPECIAL INTEREST:

Geomorphology

PROFESSIONAL EXPERIENCE:

Research Assistant, Berkeley Geochronology Center, July 2014-June 2015

Research Assistant, San Francisco State University, May 2013-August 2013

ACKNOWLEDGMENTS

I would like to sincerely thank Dr. Josh Roering for his guidance, assistance and encouragement in undertaking the research for this manuscript. I would also like to thank members of the Department of Earth Sciences community who were particularly helpful in facilitating the completion of this work, including Drs. Alan Rempel, Leif Karlstrom, Paul Richardson, and Dustin Carroll, as well as Matthew Morriss and Dan O'Hara. Dr. Edmund Medley was also very helpful in understanding the nature of antisocial mélanges. This investigation was supported by a grant from NASA, NNX15AR59G, to Dr. Josh Roering at the University of Oregon.

Dedicated to my parents, Patty Bonsall and Mark Shaw

TABLE OF CONTENTS

Chapter Page

LIST OF FIGURES

Figure Page

LIST OF PHOTOS

Photo Page

CHAPTER I

INTRODUCTION

Gully and Earthflow Processes

In areas of rapid tectonic uplift, rivers incise downward to keep pace with dropping base level, which in turn steepens surrounding hillslopes. As hillslopes approach their angle of repose, they become prone to mass failures of different sizes and rates, dependent upon local geology and climate. These hillslope failures, as they convey large quantities of material downhill, alter the geometry and sediment transport capacity of fluvial channel networks (Bennett et al, 2016; Oguchi, 1997; Santangelo et al, 2013; Swanson et al, 1985). This is apparent in the high order channels into which slides deliver sediment, leading to damming, channel pinning and armoring (Golly et al, 2017; Korup, 2005; Sutherland et al, 2002). It is also apparent in the organization of headwater, low-order streams that slides advect mass *through*, as mass movement can completely rework or obliterate channels on affected hillslopes. It is often difficult to quantify the interplay and evolution of fluvial and hillslope processes in areas of rapid tectonic uplift, but understanding how their morphologies coevolve is crucial in constraining hazards, informing environmental management practices and understanding general landscape evolution in areas of high uplift.

For this study, we investigate the interplay between slow-moving landslides, or earthflows, and the low-order gullies that dissect them. Earthflows is this region are primarily slow-moving (fractions of meters to several meters a year), translational bodies of colluvium, generally over ten meters thick, with a basal translational shear boundary, similar to a glacier (Handwerger et al., 2013). This basal boundary is generally irregular and undulatory, a geometry which governs the surface morphology of the earthflow surface. Earthflow morphology exerts a strong control on the organization and behavior of gullies, both by forcing channels to the margins of the earthflow body, and by forcing channels to navigate the irregular topography created by the basal shear boundary.

Gullies are immature erosional fluvial channels, often linear in their planform geometry, with steep banks and headwalls. Gullies generally form as a response to a significant environmental or hydrological change that allows rapid incision into soil or weathered bedrock. They typically propagate uphill during large runoff events, and incise into low or planar slopes through headwall undercutting, collapse and bank failure (Rengers and Tucker, 2014; Knapen et al, 2007). Poesen et al (2003) found that gully heads stop retreating and gullies stabilize once upstream drainage area diminishes enough such that flows no longer exceed critical shear stress for transport of soil, and Rengers and Tucker (2014) suggest that vegetation change can halt headwall migration.

Many studies have focused on gully formation in areas of agricultural overtillage (Gordon et al, 2008; Sidorchuk and Golosov, 2003; Valcarcel et al, 2003; Vandaele and Poesen, 1995;, Zhang et al, 2007), human alteration of soil grain size (Nyssen et al, 2001), deforestation (Burkard and Kostaschuk, 1995; DeRose et al, 1998; Marden et al, 2005; Parkner et al, 2006; Stankovianksy, 2003), and wildfire (Moody and Kinner, 2005; Wondzell and King, 2003). Very few studies, however, have investigated channel development in response to hillslope mass movement. Those that have are often in a secondary, cursory manner (Parkner et al, 2006; Mackey and Roering, 2011) or do not incorporate time-dependent processes (Santangelo et al, 2013, Oguchi, 1997). As such, little is known about the morphologic evolution, distribution, or sediment transport role of nascent fluvial channels that are often observed in landscapes recently disturbed by mass hillslope movement.

We focus on gully networks in a zone of high uplift, within the Central Fork Eel River basin, in the Coast Range of Northern California. We compare channels in this area to more tectonically quiescent zones in the South Fork Eel and Russian River basins. Due to high uplift and weak bedrock, the vast majority of our Central Fork focus area is subject to pervasive earthflow-like slope failures, or exhibits evidence of past failure. It is also densely dissected by low order channels. In our study area, we observe that channels coupled to earthflows are often immature, with steep, failure-prone banks. They also often become disconnected as they navigate the undulating and hummocky topography characteristic of earthflows in this area, forming alluvial fans in low-slope areas, and

incising into areas with higher slope. Conversely, channels on stable slopes (most often relict or dormant earthflows) exhibit more diffuse and stable banks, and have coherent, connected channels. This landscape stands in contrast to areas of the same rock type farther south in the Eel River basin, where channel densities are much lower and slope failures are non-existent or trivial.

While the sediment flux and rate of movement of the earthflows have been constrained (Roering et al., 2015; Bennett et al., 2016), the relative sediment contribution and morphological evolution of the gullies that dissect them remain poorly understood. In this study, we aim to clarify the influence of hillslope mass wasting on fluvial network organization and morphology in tectonically active areas, as well as the role that uplift and coincident landsliding play in dictating channel density and organization across different tectonic regimes. First, we analyze the distribution and morphology of channels in three study sites of the same rock type, with different tectonic uplift signals. We then focus closely on the evolution of channels between different stages of earthflow movement and inactivity, examining the change in longitudinal form of channels as they navigate over and incise into the irregular and dynamic earthflow surface. Finally, we utilize the presence of low-slope alluvial fans on earthflows to estimate a lower-bound sediment flux for channels coupled with active earthflows. Our findings reveal facets of the interplay between accelerated hillslope and fluvial processes in active tectonic settings, specifically the capacity of mass failures to enable the formation and dictate the morphology of low-order channels.

Study Area: Northern California Coast Range

The tectonic regime of the Northern California Coast Range is dominated by the northward migration of the Mendocino Triple Junction (MTJ), where the subduction interface of the Gorda and North American plates meets the strike-slip boundary of the Pacific and North American plates (figure 1). The right-lateral San Andreas Fault "pushes" the subducting Gorda plate northwards at 5 cm/yr, opening a slab window to the southeast of the MTJ. This promotes crustal flow and subsequent crustal thickening, resulting in rock uplift of >1 mm/yr within our main study area in the Central Eel River

drainage (Furlong and Gover, 1999; Lock et al, 2006). This also results in crustal thinning and corresponding subsidence farther South in the Russian River basin.

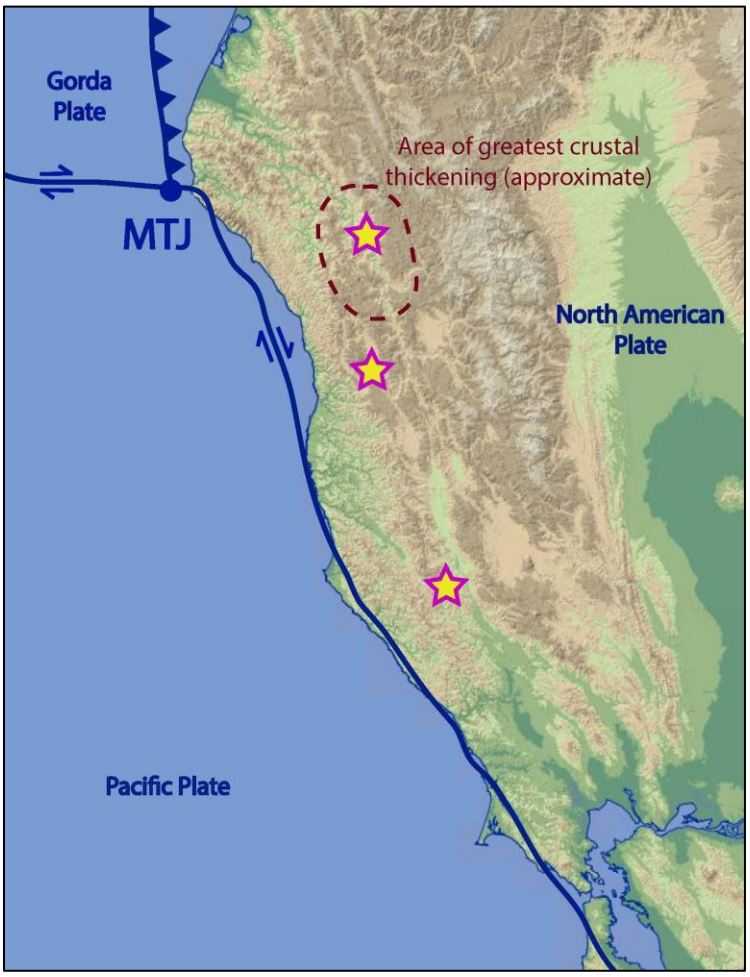

Figure 1: Our three study areas, in relation to the geography of Northern California and the Mendocino Triple Junction (MTJ). As the subducting Gorda Plate is pushed northward by the San Andreas Fault, lithosphere and asthenosphere flows into the vacated space, resulting in crustal thickening and isostatic uplift.

The lithology of the Northern California Coast Range is dominated by the Franciscan Complex - a Jurassic-Cretaceous accretionary prism, sheared, metamorphosed and uplifted since the Miocene following accretion during oceanic subduction. The Franciscan Complex is separated into three separate belts: the Eastern, Central and Coastal. These belts trend South-North and decrease in age towards the West in accordance with their accretion to continental North America (McLaughlin et al., 2000).

Our study area lies within the Central belt, which is prone to pervasive slope failure due to a weak bedrock matrix of sheared argillite. Contained within this matrix are more competent metamorphic rocks - primarily greywacke, with blueschist, greenstone, chert and serpentinite. These harder clasts vary in size from pebbles to mountain-scale (10^{-2}-10^{4} m), and are distributed seemingly randomly throughout the argillite matrix. Medley (1995), however, found that these harder clasts are actually fractally distributed within the Franciscan mélange - that is, their spatial distribution and size proportions are invariant relative to the scale at which they are sampled. The harder metamorphics are very important in governing local landscape dynamics - large "megaclasts" set topographic highs, and relatively smaller rocks dictate the basal geometry of earthflows, as well as fluvial incision and geometry by composing bedload in channels and creating armored knickpoints in Eel tributary reaches (Bennett et al, 2016).

The vast majority of sediment exported from the Central Franciscan and the Eel is derived from the sheared argillite matrix, which is readily converted to soil and transported as suspended load. Brown and Ritter (1971) established that the Eel River has the highest suspended sediment load per unit drainage area of any river its size or larger in the United States, and that the highest proportion of sediment originates in areas dominated by landsliding. Roering et al (2015) further clarified that over half of suspended sediment yield is attributable to the intersection of earthflow toes with perennial streams within the zone of high uplift. In this study, we compare three LiDAR DEMs within the Central Franciscan Complex, each with a different uplift rate, and then focus on processes within our northernmost DEM, where uplift is greatest. Our southernmost DEM is near Yorkville, CA, in the Russian River watershed, and lies within the area of crustal thinning (figures 2, 3, and 4). Ferrier et al. (2005) compute an erosion rate of 0.09mm/yr in the nearby Casper Creek watershed. We also analyze a DEM near Branscomb, CA (figures 5, 6, and 7), which has a calculated erosion rate of 0.22mm/yr (Willenbring et al., 2013). Both of these DEMs were obtained from Open Topography (opentopography.org) and clipped to analyze only sections within the Central Franciscan Belt, as mapped by the USGS. Our primary DEM (figures 8, 9, 10,

and 11) lies farther to the North, and is in the focus of tectonic uplift from the MTJ. Airborne LIDAR was flown by NCALM in 2006.

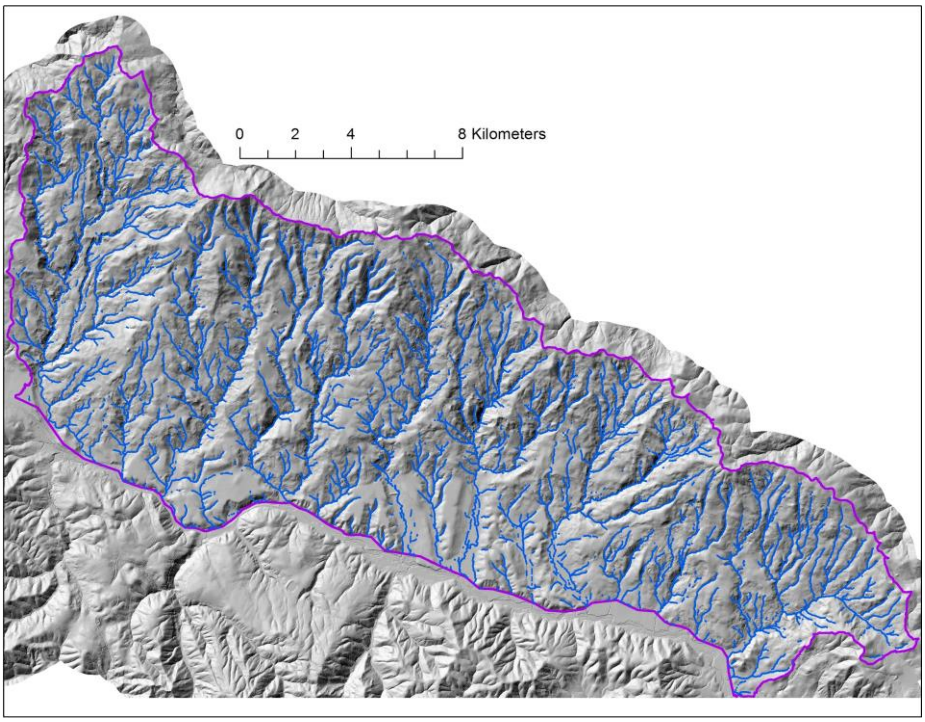

Figure 2: Southernmost DEM, near Yorkville, CA. This lies within the Russian River watershed. The purple line delineates the edge of the area we analyze, and blue lines represent stream channels derived from geonet. Geographic coordinates: 38°54'17.88"N, 123°10'4.59"W

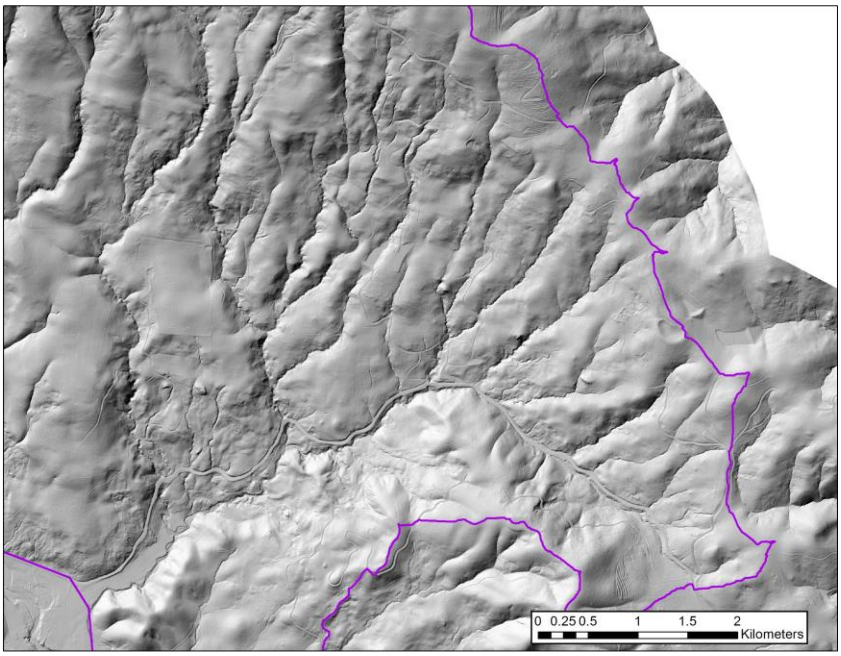

Figure 2: Yorkville DEM, zoomed view, SE corner. Channelized areas are more widely spaced (note scale) and hillslopes are texturally smooth and diffuse.

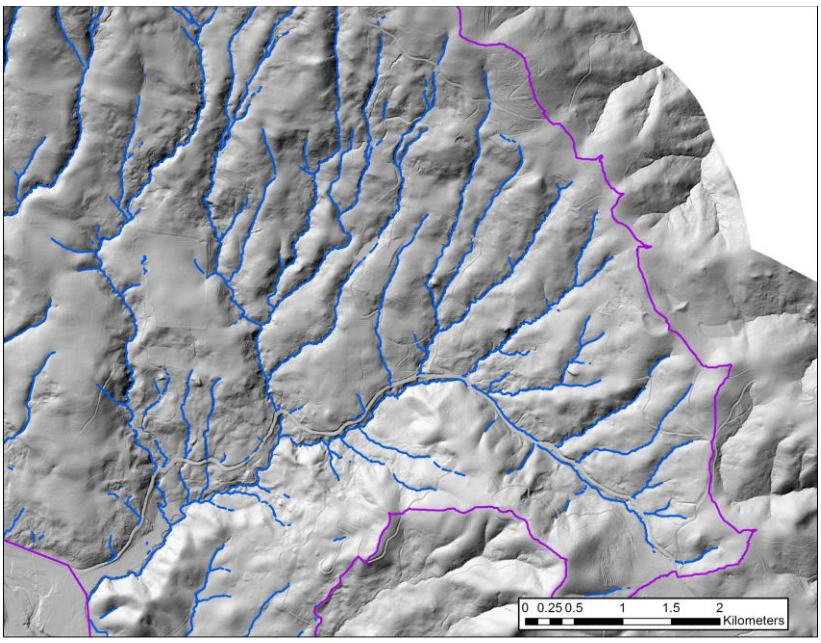

Figure 4: Yorkville DEM, zoomed view with channels. Almost all channels are completely continuous, networks are well organized.

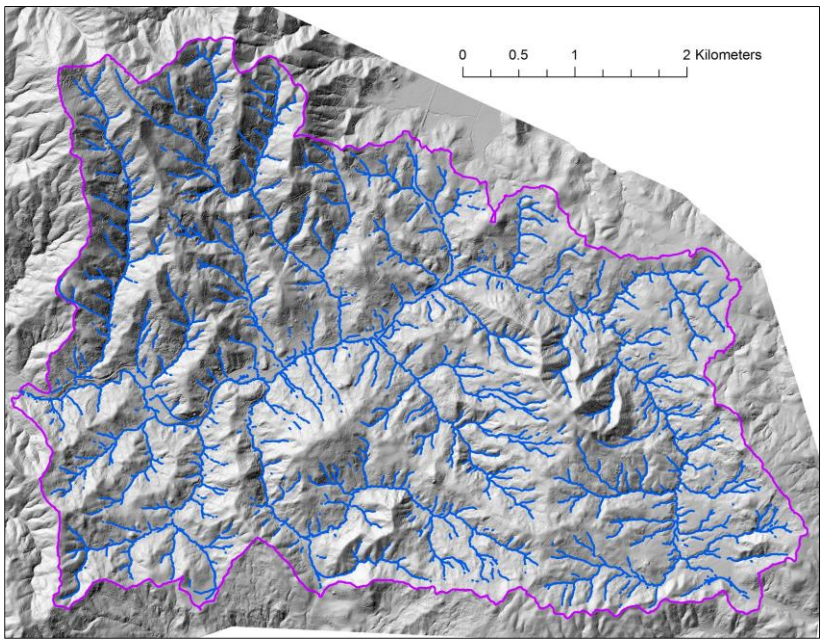

Figure 5: Middle DEM, southeast of Branscomb, CA. The purple line delineates the edge of the watershed we analyze, and blue lines represent stream channels derived from geonet. Geographic coordinates: 39°37'19.40"N, 123°31'28.08"W

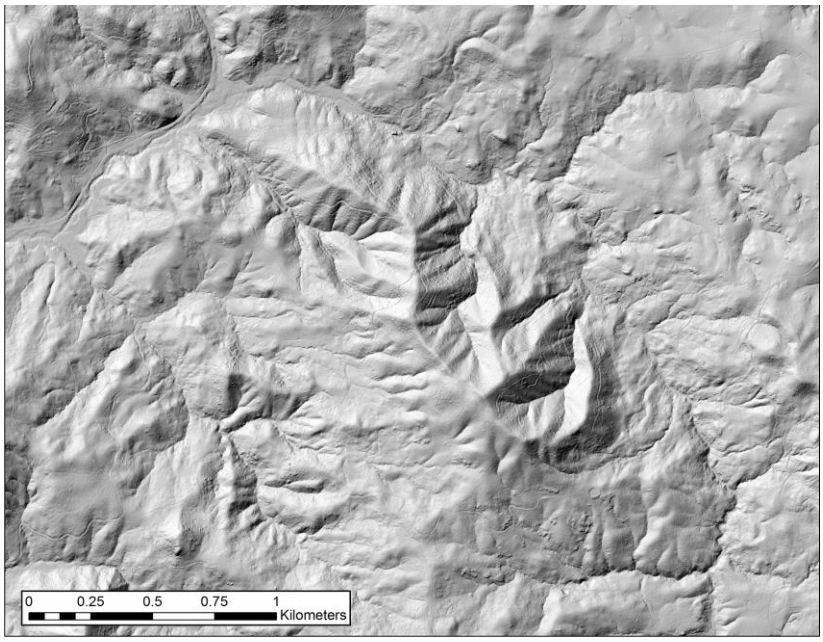

Figure 6: Branscomb DEM, zoomed view, NE corner. Area shown is well dissected with channels. The higher, deeply incised area in the middle of the image is likely a very large metamorphic "megaclast," creating a topographic high with steeper, more incised channels.

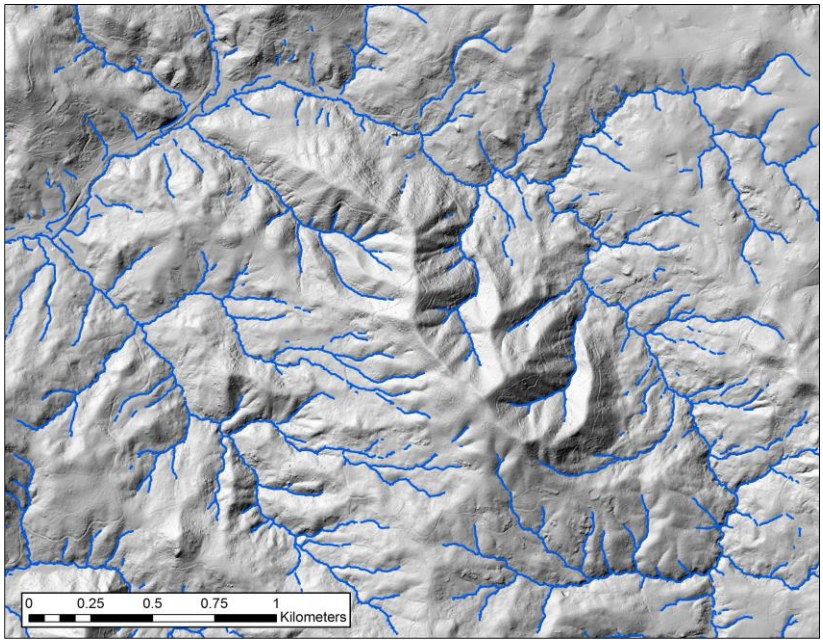

Figure 7: Branscomb DEM, zoomed view with channels derived from geonet. Most channels in the image are continuous. Networks are heirarchical well-organized.

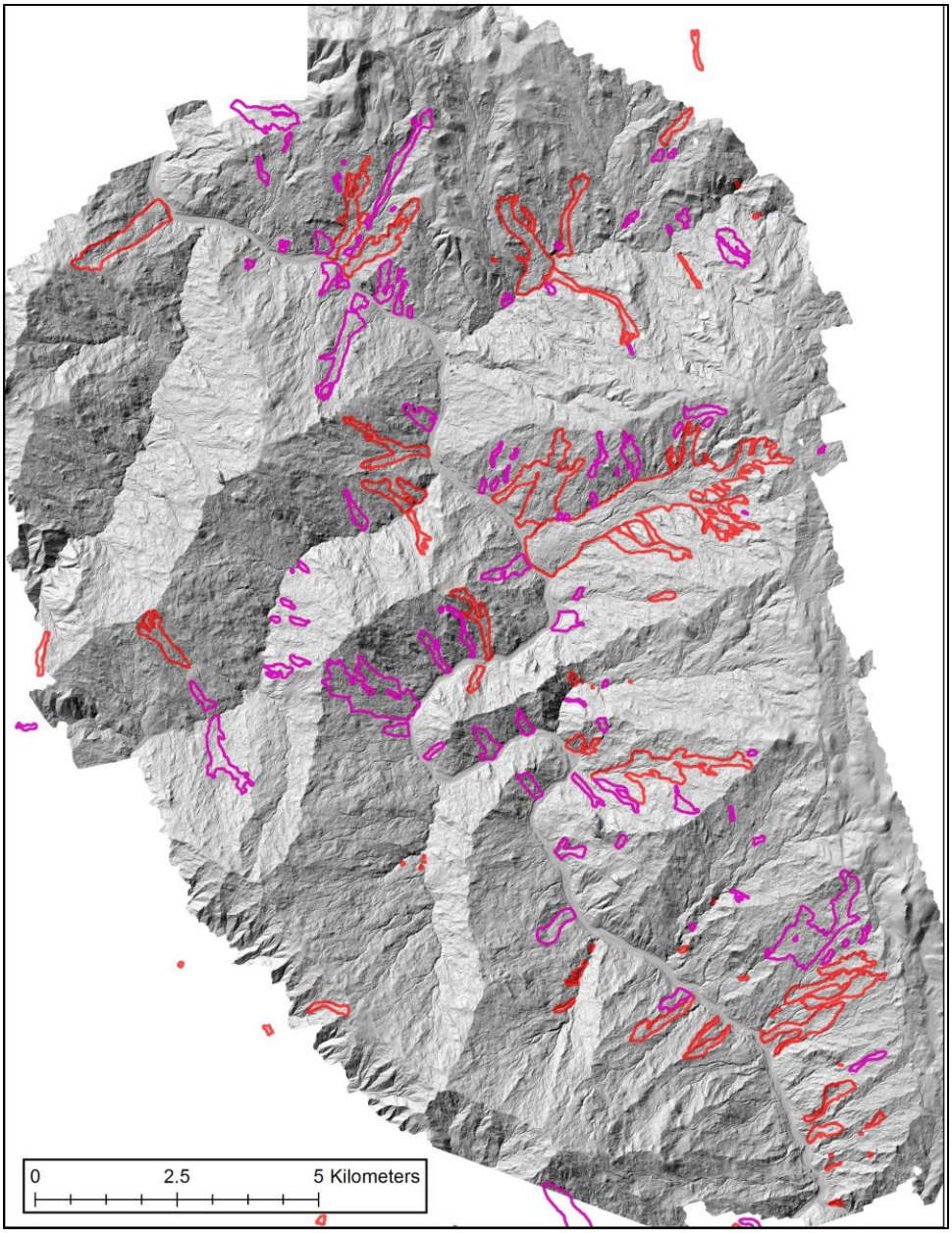

Figure 8: Northernmost DEM, just south of Alderpoint, CA. The Central Fork run south to north through the middle of the DEM. Red polygons denote active earthflows, and pink polygons denote dormant earthflows. Note the hummocky topography and relict headscarps throughout the area, even where there are no mapped slides. Geographic coordinates: 40° 5'38.12"N, 123°29'45.84"W

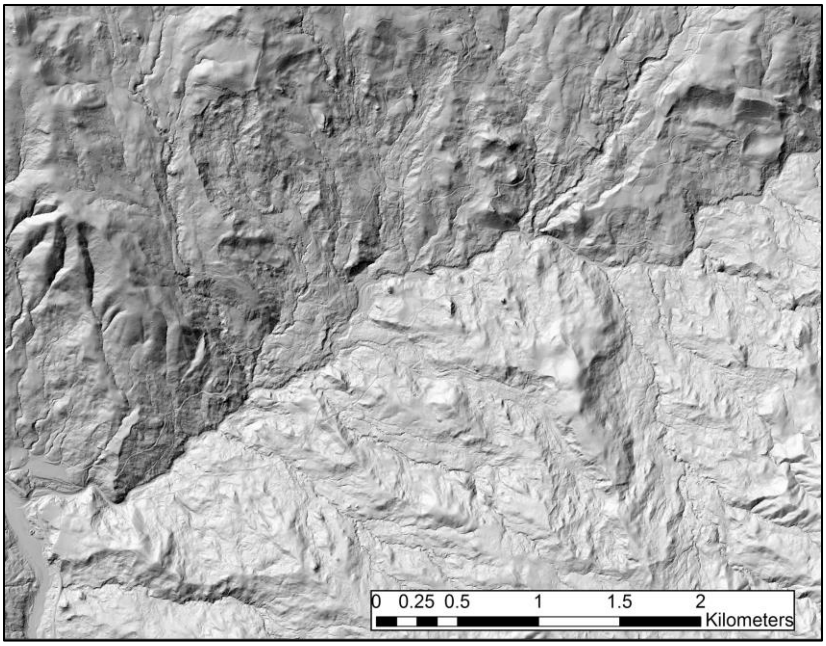

Figure 9: Hillshade map of the Kekawaka Creek watershed, where all field measurements and observations for this study were made. Kekawaka Creek runs from NE to SW in this image, and joins the Central Fork Eel River in the lower left, which runs South to North. Note the highly disrupted and hummocky topography across several scales in the image.

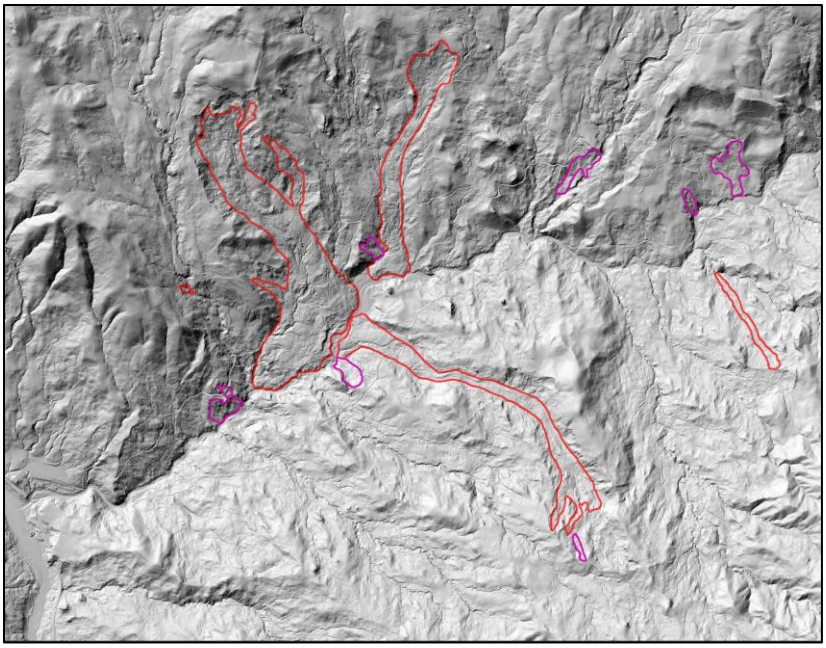

Figure 10: Kekawaka Creek watershed with earthflows. The large active earthflows (red), clockwise from the rightmost earthflow, are the Two Towers slide, Penstock slide, Fatty slide, and Kekawaka slide.

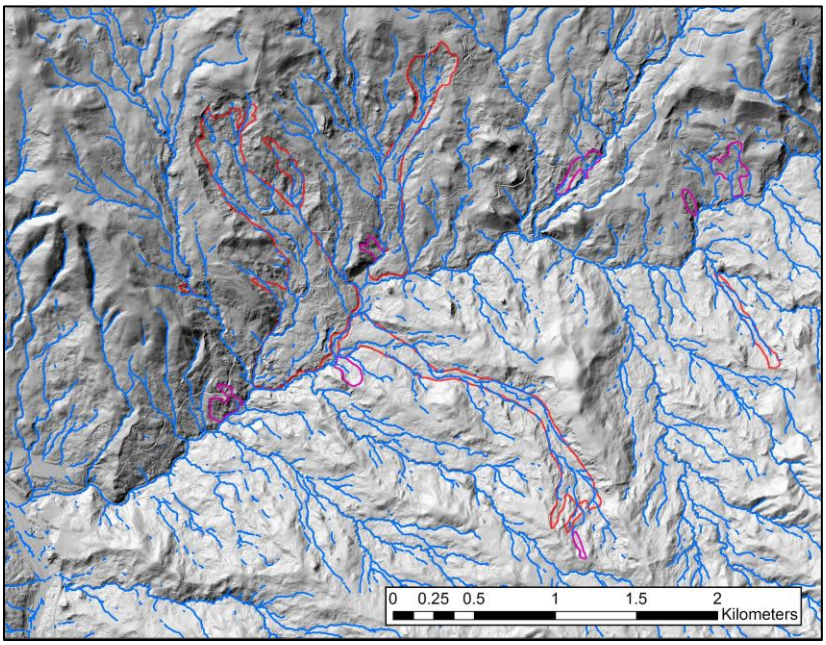

Figure 11: Kekawaka Creek watershed with channels. Networks are highly disrupted, but the channel density is very high.

CHAPTER II

OBSERVATION AND ANALYSIS OF CHANNELS

Methods

Using Geonet to extract channel networks

To assess the extent and spatial distribution of gullies, we required a tool to automatically extract channels from DEMs. This is often accomplished with a workflow that consists of 1) filling sinks or depressions in the DEM, 2) computing steepest descent flow direction between raster cells, 3) computing flow accumulation, 4) assigning catchment outlets and 5) determining channel head locations based on a flow accumulation area value. This workflow often yields acceptably accurate channel locations in well-dissected and fluvially dominated landscapes. However, the sink-filling protocol and steepest descent approach would not honor the hummocky landscape and disrupted channels we observe for gully prone hillslopes in Northern California. A different method was needed that would recognize locations where channels terminate and reform midslope. To determine channel locations, we used the channel extraction program *Geonet* (Passalacqua et al., 2010, Sangireddy et al, 2016). Instead of employing steepest descent to determine channel locations, Geonet uses non-linear filtering to remove small-scale variations, then extracts likely channelized pixels based on local curvature values to determine channel banks. In other words, this algorithm maps channel banks rather than assuming that channels exist at sufficiently large drainage areas and follow the steepest descent without exception.

Geonet has a small number of computational parameters that can be specified by the user to alter the extent of predicted channelized areas. In order to determine which values to use in determining channels over our entire DEM area, we compared several Geonet iterations of differing parameter values against channels mapped within our study area by field observations and handheld GPS. We adjusted two parameters from the

original default values provided in the original Geonet code (https://sites.google.com/site/geonethome/source-code): the DEM Smoothing Quantile parameter and the Flow Threshold for the channel skeleton. The smoothing quantile - which determines how much convexities within the DEM are smoothed out versus how much they are enhanced - we set to a value of 0.3. We determined that this best captured shallow low order channels that we mapped, which were not captured with higher smoothing quantile values. We set a flow threshold value at 6000 pixels, or 6000 m^2 upstream drainage area.

The above parameters were chosen by visually comparing Geonet results from multiple value iterations to ground-truthed channel locations, mapped in the field with handheld GPS. We primarily mapped channels on two earthflows, the Kekawaka and Fatty earthflows (Mackey and Roering, 2011). We used a Trimble GeoXH 2008 handheld GPS and walked along channels until we reached gully headcuts or channels were no longer distinguishible. Small interferences in completely mapping channels included overhead satellite interference from trees, as well as poison oak growth. All channel locations had a location error of less than one meter. Geonet channels did not exactly match GPS channel locations (and we would not expect them to in such disrupted terrain), but they did satisfactorily capture channel interruptions.

In order to perform analysis on geonet channel rasters, we had to convert them to polylines. To accomplish this, we intersected geonet results with flow accumulation within ArcMap, according to the following workflow (figure 12):

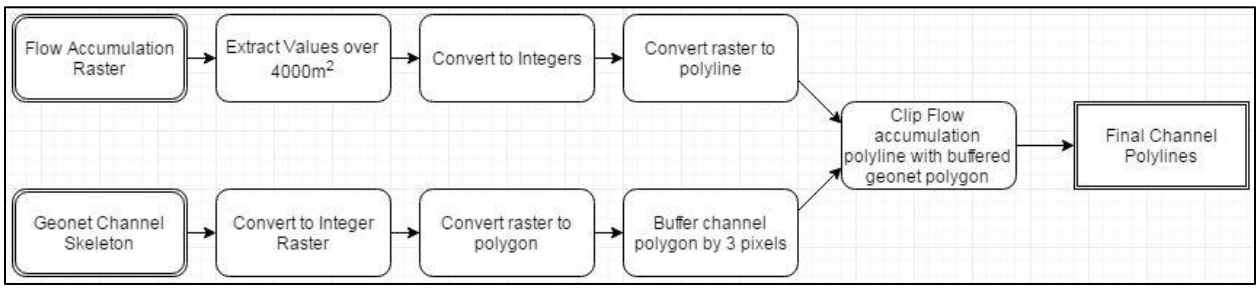

Figure 12: workflow for obtaining geonet channel polylines

Steps:

1a. Create flow accumulation raster

2a. Extract values over 4000m^2 for use (discard values under 4000m^2)

3a. Convert flow accumulation values to integers.

4a. Convert flow accumulation raster to polylines.

1b. Import binary Geonet channel skeleton (.tif format) into ArcMap as binary raster.

2b. Convert to integer raster, change background value of 0 to NoVal.

3b. Convert raster to polygon.

4b. Buffer the polygon by 3 pixels on all sides.

5. Use the Clip tool to extract flow accumulation polyline bounded within the buffered geonet polygon.

6. Final result of polylines with accurate channel interruptions (figure 13).

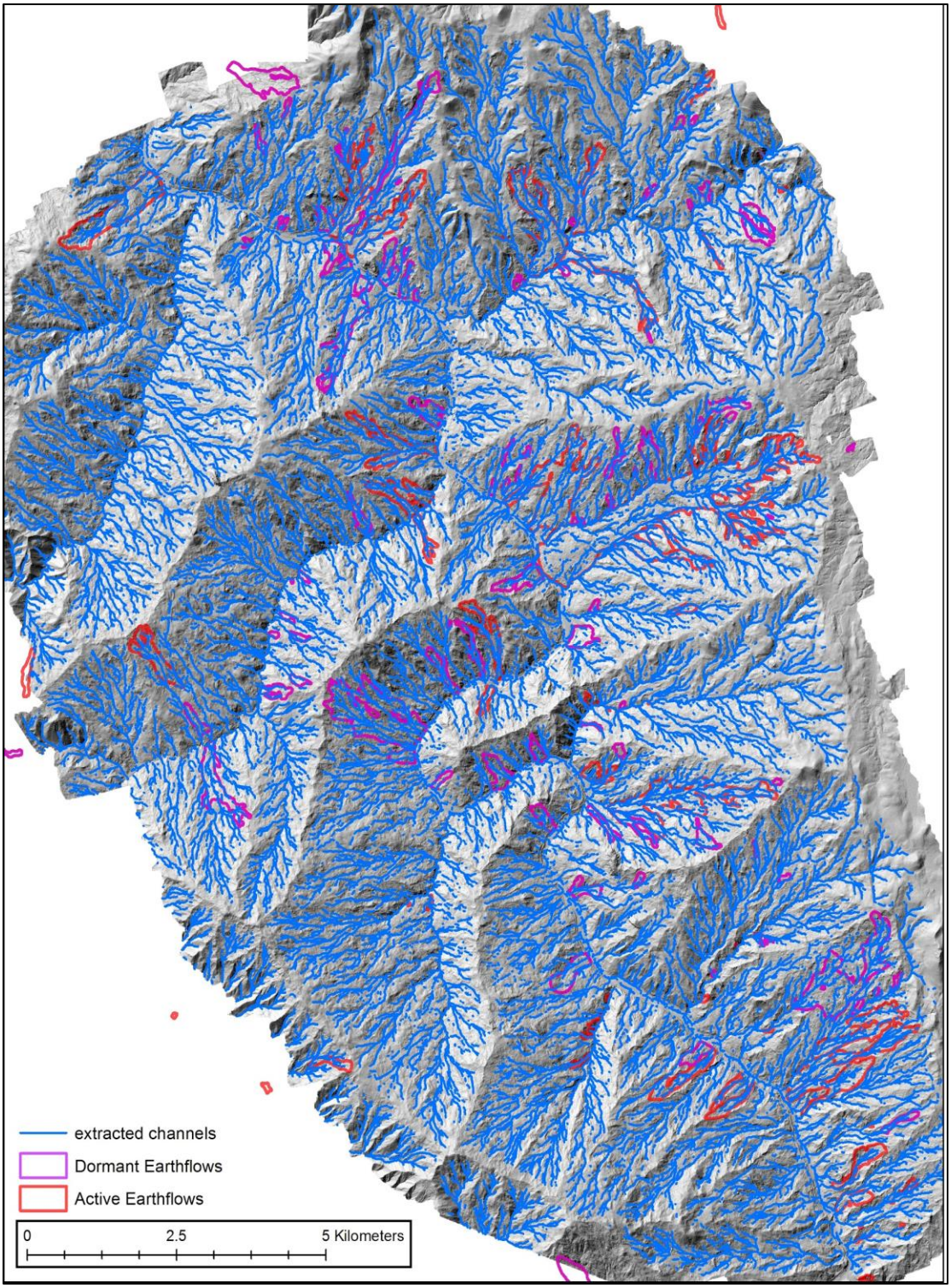

Figure 13: Central Eel DEM, with geonet-derived channels. Note the high drainage density in comparison to the other two DEMS.

Comparing Drainage Density Across Tectonic Regimes and Earthflow Activities

After extracting channels within our three DEMs, we use our channel polylines to determine the total drainage density of all three DEMs. Drainage density is defined as the total length of channels within a basin, divided by the basin area. Differences in drainage density between drainage basins can be due to a variety of reasons, including precipitation, infiltration capacity, and physiographic relief. Here, we investigate differences in drainage density as related to variations in tectonic uplift, and by extension, erosion rates, assuming an approximate balance between tectonic forcing and geomorphic response. We infer local erosion rates for our southern DEMs from two studies: Willenbring et al (2013) and Ferrier et al (2005). Both studies use cosmogenic nuclide measurements to determine erosion rates at similar latitudes to our two study sites. WIllenbring et al (2013) calculate local exhumation near Branscomb,CA to be 0.22 +/- 0.02mm/yr. Ferrier et al (2005) calculate and exhumation rate of 0.09 +/- 0.02mm/yr within Caspar Creek, CA, which is at a near-equal latitude and uplift gradient to our site near Yorkville, CA. Finally, erosion rate within our main northern study area is 0.9 +/- 0.3mm/yr (Wheatcroft and Sommerfield, 2005). Since the tectonic uplift gradient in this area trends north-south (Lock et al, 2006), we also plot drainage density against latitude as a proxy for local uplift.

In addition to comparing drainage densities between our three study areas, we also investigate the evolution of drainage density as active earthflows within our primary study area become dormant, and then stop moving entirely. To do this, we separate dozens of topographic hollows into three categories: active, dormant, and inactive (figure 14) . All active, and most dormant earthflows were identified by Mackey & Roering (2011), as well as Bennett et al (2016). Both active and dormant earthflows exhibit typical earthflow morphology: amphitheater-like headscarps, hummocky and disturbed terrain, and often levees and lobes. These researchers used historical aerial imagery (1940-2006) to distinguish active slides from dormant slides. Active slides translated trees and bushes downslope, whereas features on dormant slides remained static. We delineated inactive convergent zones as those that show no recent signs of earthflow activity. Headscarps, if they exist, are diffuse, and the valley has been fully incised to

make a v-shaped cross-section, with a central channel and dendritic channel network. In comparing drainage densities between these zones, we sum the total channel length within each, as derived from geonet, and divide by the earthflow or convergent zone area.

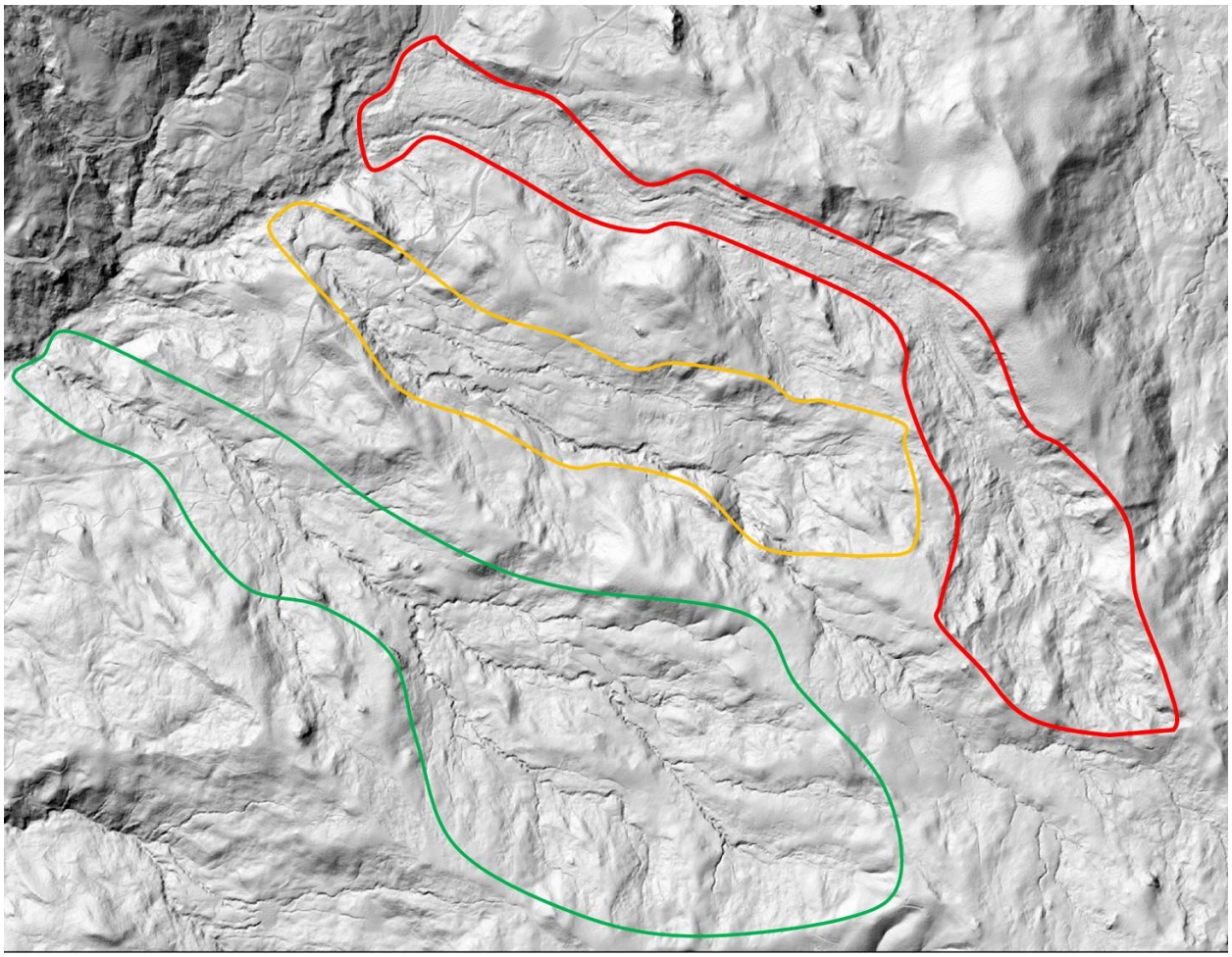

Figure 14: The active Penstock flow (red), a dormant flow (yellow), and an inactive convergent zone (green). The inactive zone is dissected by an axial channel down its center, and has a more classically dendritic channel network. The dormant flow is more diffuse than Penstock flow, but still has lateral channels and an infilled valley. The Penstock flow shows signs of movement, has a disrupted surface, and a spreading toe, which deposits into Kekawaka creek to the Northwest.

Curvature of Channel Profiles

Field observations of earthflow-coupled gullies, as well as a qualitative assessment of their longitudinal profiles, suggest that gully morphology is slave to earthflow movement during earthflow activity. Gullies do not incise deeply into earthflows, especially at lower drainage areas, and exhibit similar profiles to earthflows -- that is, they undulate between steep and gentle gradients around a linear low-slope (~20 degree) trend (figures 15, 16, 17). This behavior differs greatly from normally behaving stream channels, which generally exhibit a concave-upward profile (or positive curvature), steepening with increasing elevation. In order to assess whether these unusual gully profiles are due to earthflow activity, we examine the local curvatures of trunk streams coupled with active, dormant, and inactive flows, as described previously. Specifically, we examine differences in curvature variance over local scales, as high variance in curvature would indicate changes between high and low slopes. Examining differences in the variance of curvature (or the second derivative of the channel profile) between channels on moving earthflows (active), channels on relatively recent earthflows (dormant), and areas that have not experienced mass failure in a significant amount of time (inactive), can lend insight as to the evolution of channels once earthflows shut off, and channel incision and fluvial transport becomes the primary erosional process. If channels are able to incise into convexities and deposit into concavities created by the earthflow, they will act to "dampen" undulations in their profile, and will decrease variance in their profile curvature. Since an idealized, steadily eroding channel would display a consistent concave-upward profile with little local variation in curvature, we would expect channels in inactive zones which have been actively incising to display less variation in local curvature over scales relevant to the undulating topography of an earthflow.

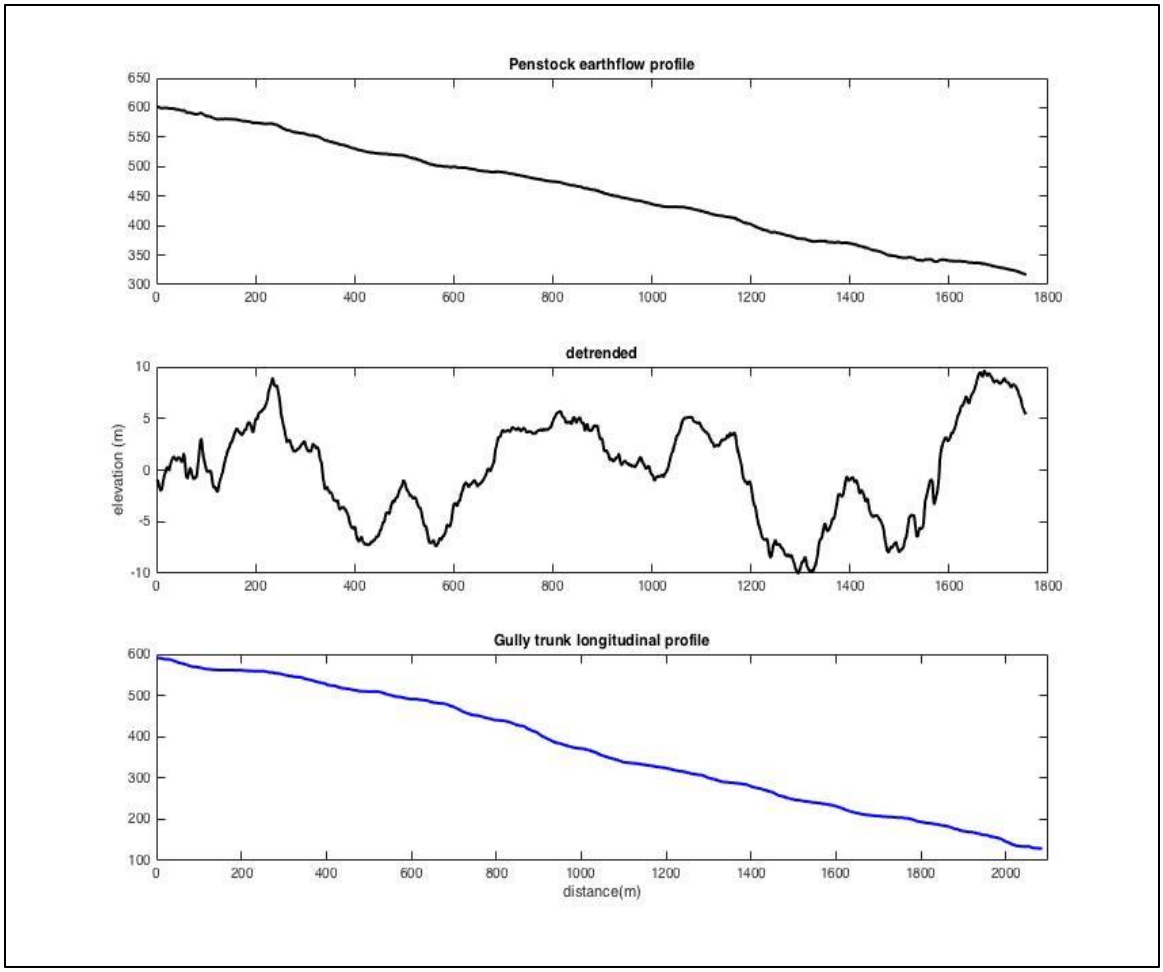

Figure 15: Penstock slide earthflow profile, with slope and detrended, and the longitudinal profile of the gully trunk channel paired with it. Note the similarities in slope and undulations between the two.

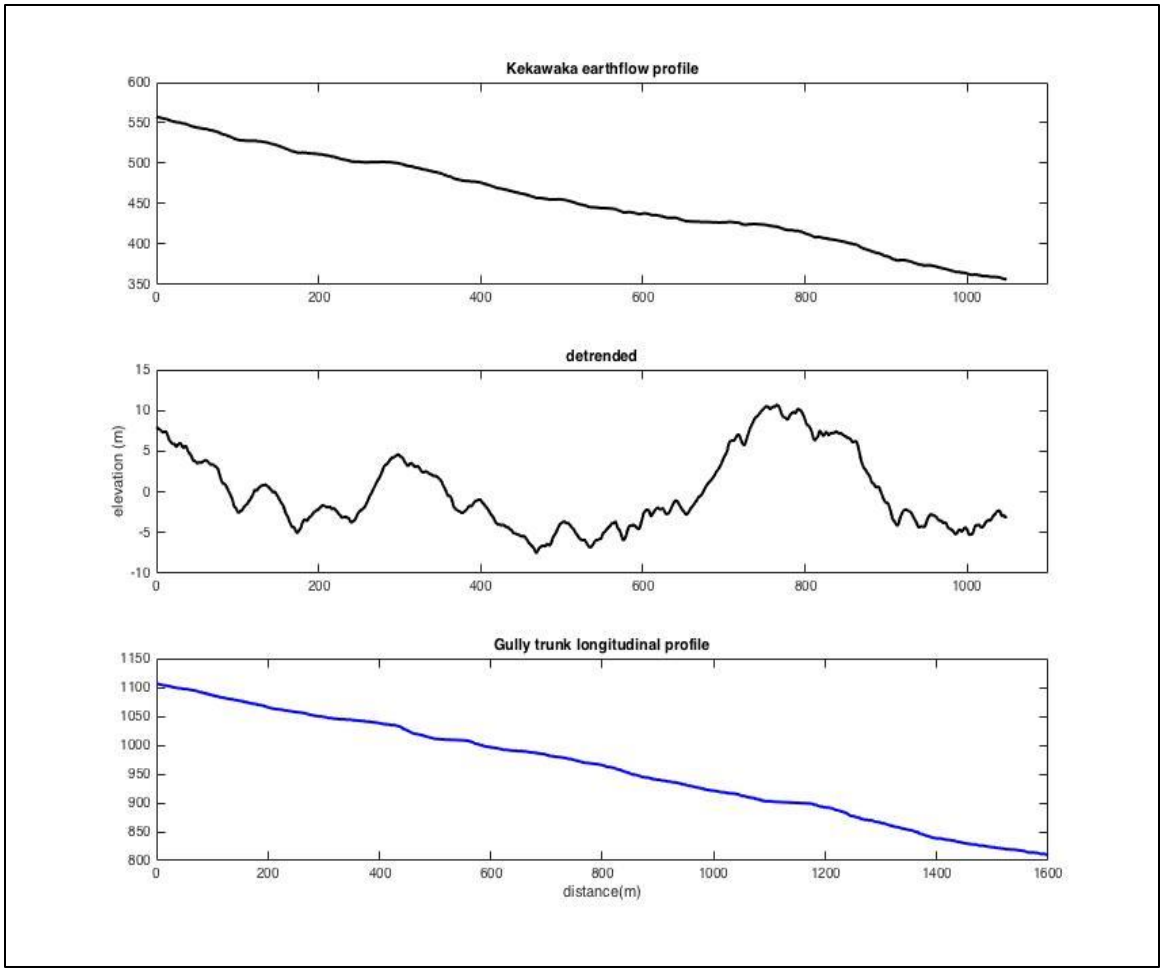

Figure 16: Kekawaka slide earthflow profile, with slope and detrended, and the longitudinal profile of the gully trunk channel paired with it. Note the similarities in slope and undulations between the two.

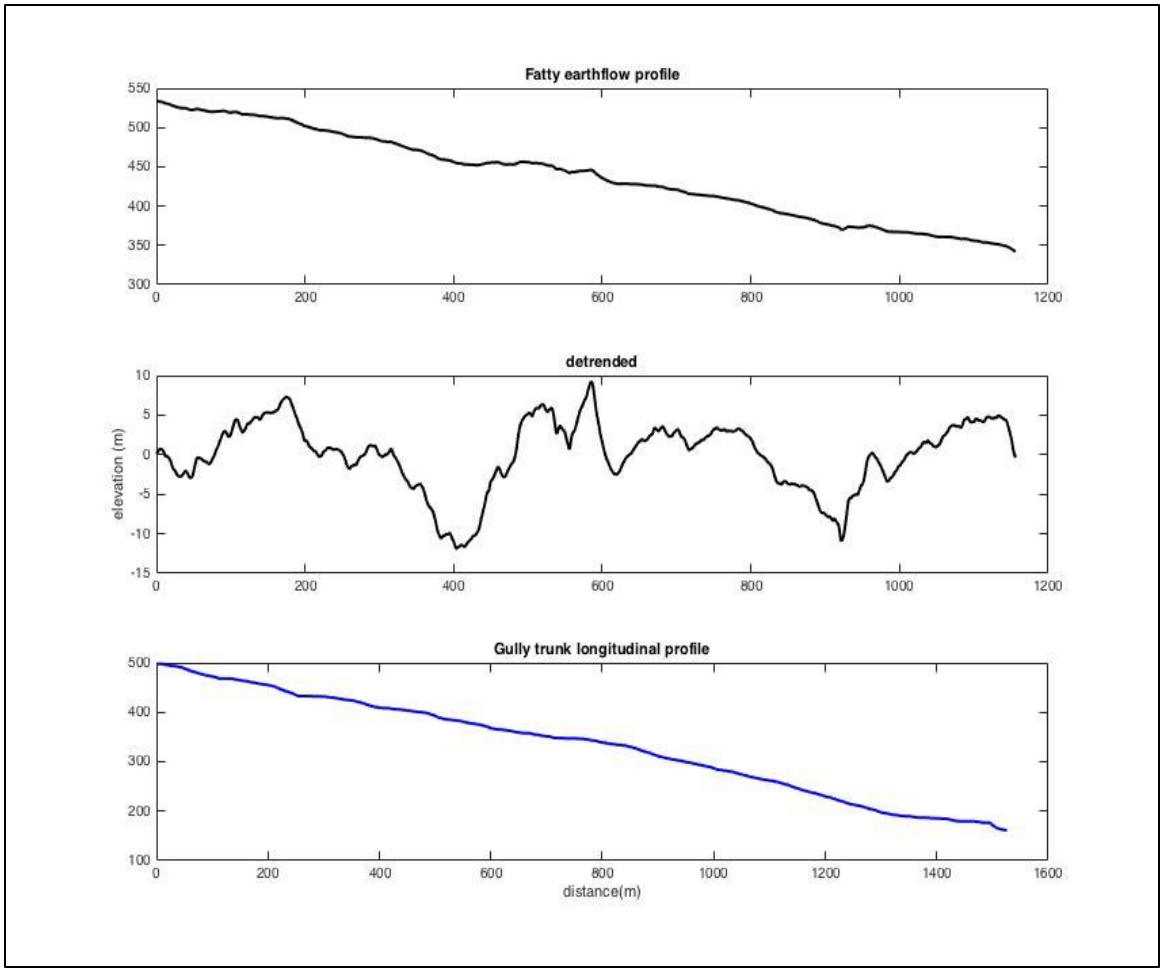

Figure 17: Fatty slide earthflow profile, with slope and detrended, and the longitudinal profile of the gully trunk channel paired with it. Note the similarities in slope and undulations between the two.

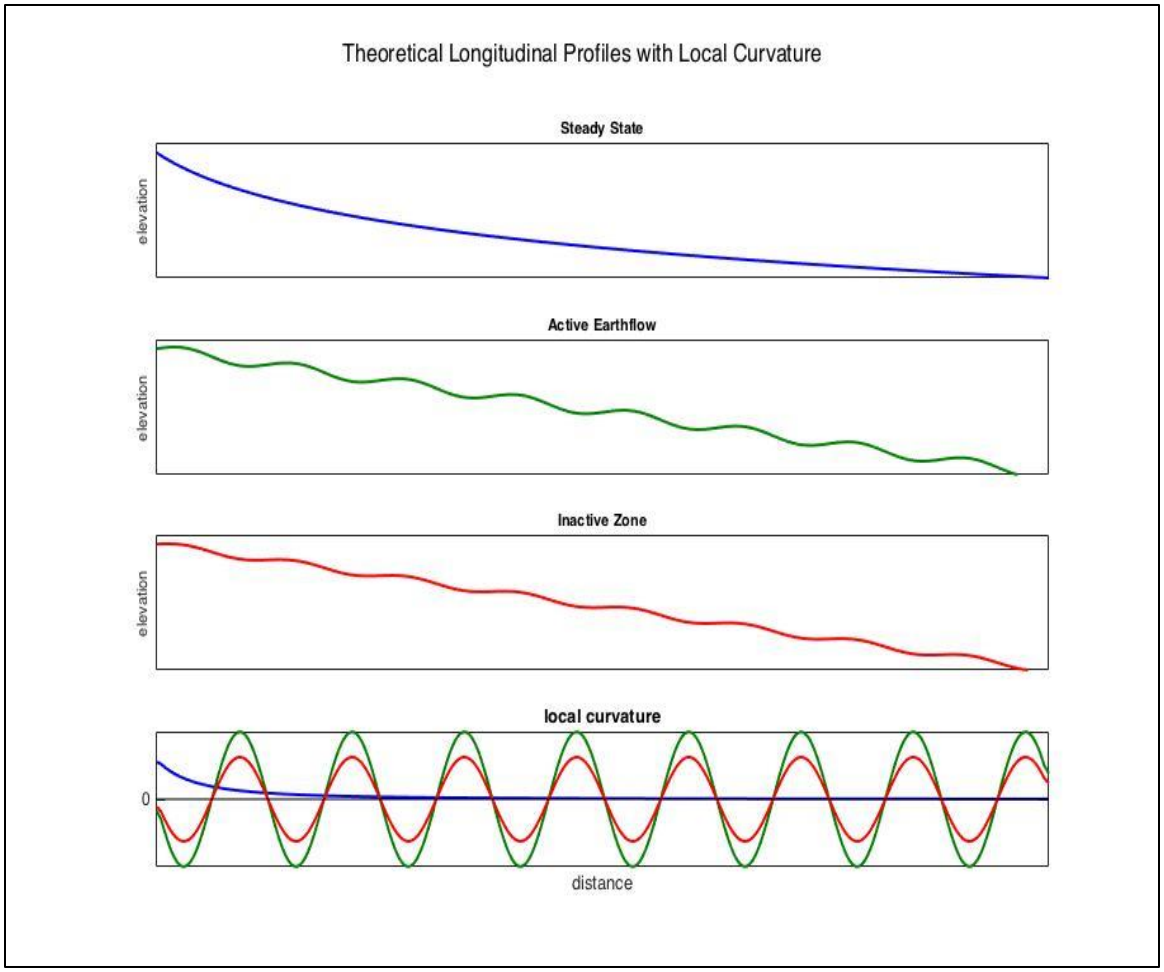

Figure 18: Long profiles of three different theoretical channel types -- steady state, active earthflow, and inactive zone -- and their corresponding curvatures. Inactive channels, which have a suppressed undulations in this case, also exhibit lower variance in curvature than active channels.

First, we chose outlets of low-order channel networks coupled with active flows (n=15), dormant flows (n=22), and inactive convergent zones (n=22). We used tools by Adam Forte (https://github.com/amforte/TopoTools://github.com/amforte/TopoTools), based off the matlab functions from Topotoolbox (Schwanghart and Kuhn, 2010), to extract drainage basins for each outlet point, derive channel networks by steepest descent, and then extract the trunk stream from each channel network. We then computed local curvature for each point, using a predetermined radius over which to calculate slope and curvature for every point on the stream with a second-order polynomial. These radii

range from 5m to 300m, increasing by 5m with each iteration. This approach is intended to identify changes in curvature on scales that are smaller than, equal to, and/or larger than the scale of earthflow undulations and associated alluvial fans that channels navigate as they flow down the surface of a slide. We compute the standard deviation of curvature for each channel, within each group, for each radius of curvature fit. We then perform an ANOVA test to determine if curvature variance differs significantly between the three channel types.

Results

Geonet Accuracy

We used Geonet to extract channel locations from LiDAR DEMS of three Coast Range landscapes of Central Franciscan bedrock. Our southernmost location, near Yorkville, CA does not display any topographic signatures of mass wasting, while the middle location, near Branscomb, CA, exhibits limited and highly diffused relict features. Both are fluvially dissected in an organized, dendritic pattern (figures 4 through 7). The Geonet-derived channels from these two locations tend to coincide with channels identified by the steepest descent (or D8) flow accumulation algorithm. In our northern field site, we mapped channel locations on Kekawaka earthflow with handheld GPS (all location errors <1.0m) to compare to Geonet-derived channel locations. Overall, channel locations determined from Geonet matched GPS locations very well. The most notable differences between the two occurred in the headscarp area of the earthflow, where coalescing packages of earthflow material can create steeper, bank-like lobes as they travel downhill, which Geonet's algorithm occasionally mistakes for channel banks. These false-positive errors, however, are few. Additionally, these features were often eliminated by changing Geonet parameters, and were not incorporated with the final channel polylines, as they do not coincide with the flow accumulation lines we combined with buffered Geonet channels. Geonet was very effective in identifying breaks in

channel integration (i.e., discontinuities in the channel network). Most channel interruptions derived from Geonet coincided with alluvial fans that I observed in the field. We extend this observation to the rest of the DEM, and interpret geonet channel interruptions that coincide with low slopes to represent locations of more alluvial fans or ponds.

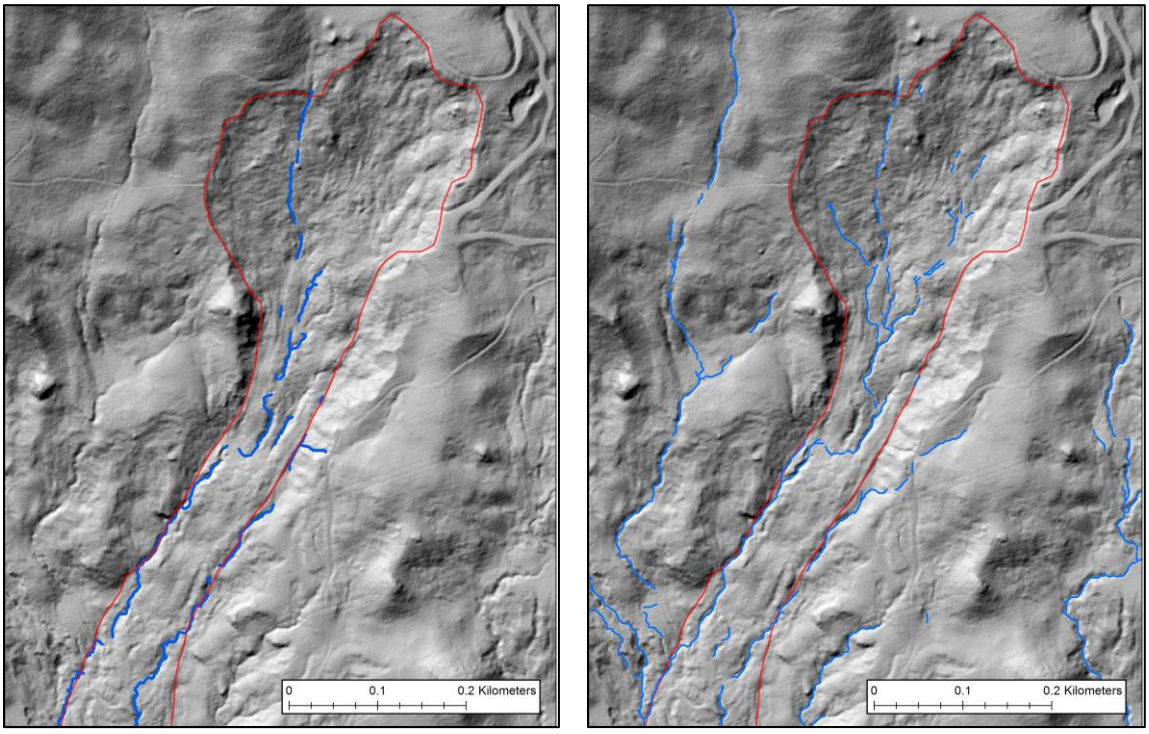

Figure 19: Comparison of GPS-mapped channels (left), and geonet-derived channels (right), on the upper half of Kekawaka slide (outlined in red).

Field Observations of Channels and Earthflows

In our field study site, the lower Kekawaka Creek watershed, we noticed several notable differences between channels in earthflow-occupied valleys and those lacking mass movement. Channel networks dominated by active earthflows featured channels that had steep banks prone to failure (photos 1 and 2). Gully longitudinal form resembles that of the earthflow, implying that channels "ride" along the earthflow surface, and do not fully incise to bedrock while flows are active. Earthflow-dominated channels showed deeper incision and steeper banks in higher-slope areas, and very shallow banks or no channel at

all where flows navigates low-slope areas. Many of these low-slope areas (where earthflow mass rides over a large convexity in the shear zone) exhibit depositional alluvial fans or ponds. Ponds appear to form in zones of lower fluvial sediment flux - fed either by gullies with very low drainage area, or fed only by the water table. Fans are always coupled with active gullies, and appear to be composed primarily of coarser sediment, compared to earthflow sediment. These fans exhibit imbrication, implying that they were deposited fluvially, and not by debris flows. Downslope of deposited alluvial fans, channels reinitiate in higher-slope sections with steep headcuts, forming deeper and steeper channel banks.

Photos 1 and 2: bank failures in a channel coupled with the Twin Towers slide (figure 10). Photos taken in late March, 2017, after heavy rain.


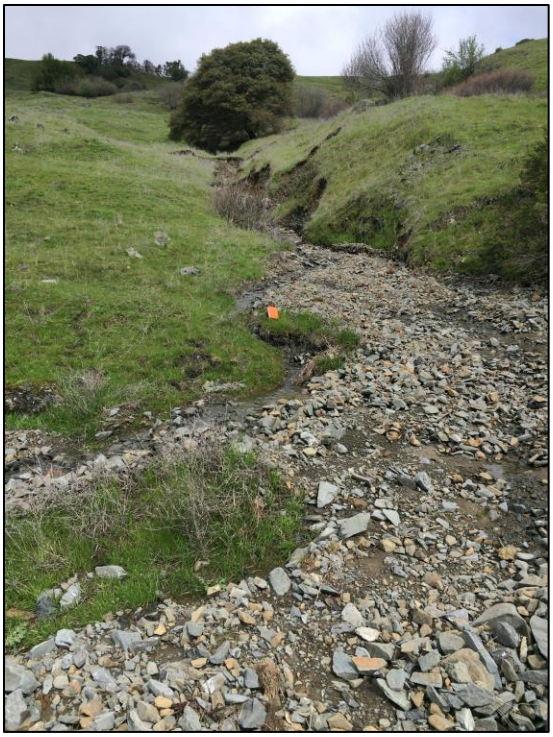

Photos 3 and 4: Examples of alluvial fans, both on Kekawaka slide. The photo on the right is looking uphill at fan 2 and the gully that feeds it. Note bank failures in the gully. The orange rectangle in the center of the photo is a standard field journal.

Channels unaffected by earthflows did not exhibit any of the unique characteristics of earthflow-dominated channels detailed above. Channel banks tended to be stable and smoother, with more established vegetation. Banks did not show the same degree of lateral bank failure observed on earthflow channels. While channels still undulated slightly, there is significant evidence of incision into areas of positive curvature. Channel beds exhibit signs of armoring, with large interlocking clasts.

Our field observations benefitted from visiting the field site before and after an above average rainfall season: the winter of 2016/2017. We were able to document qualitative changes to channels as a result of the high flows that year, which was preceded by a string of dry years and minimal earthflow movement (Bennett et al, 2016). On the Kekawaka slide, we observed no notable earthflow movement. This assessment was primarily made by inspecting a dirt road that traverses the slide halfway down, which showed no signs of displacement since the previous visit prior to the rainy season. We did, however, observe several significant changes to channels on the earthflow. Alluvial

fans were somewhat reworked, and several gully headcuts had progressed uphill into low-slope fans by several meters (photo 5). This implies that earthflow movement is necessary to counteract uphill gully headcut movement, thereby preventing channel integration by incision into low-slope areas. On the Two Towers slide, we observed many channel bank failures, which were not observed before the wet season, and were not observed in such prevalence in channels that were not coupled with active flows.

Photo 5: Photo taken in late March, 2017. Before the rainy season, the gully headcut was in the location of the bush (foreground), and has since progress several meters uphill, incising into a low-angle fan (background).

Drainage Density Results

Calculations of drainage density between the three DEMs reveal a marked increase in drainage density with increasing uplift and latitude (figures 20 and 21). We calculated drainage densities from our DEMs near Yorkville, Branscomb, and Kettenpom, CA to be $0.0023m^{-1}$, $0.0067m^{-1}$, and $0.0135m^{-1}$, respectively. These correspond to erosion values of <0.2mm/yr (Bennett et al, 2016, Ferrier et al 2005), 0.22mm/yr (Willenbring et al, 2013), and 0.7-1.1mm/yr (Balco et al., 2013).

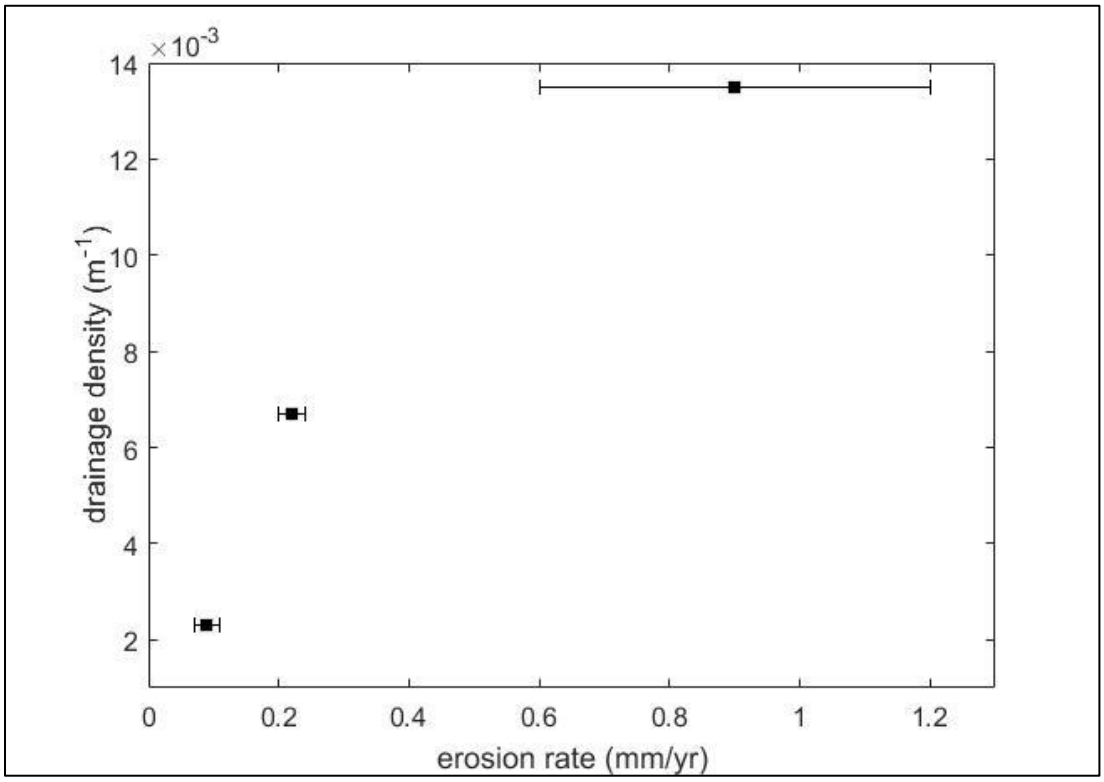

Figure 20: Calculated drainage density plotted against erosion rate in mm/yr (Ferrier et al., 2005; Willenbring et al., 2013; Balco et al., 2013),

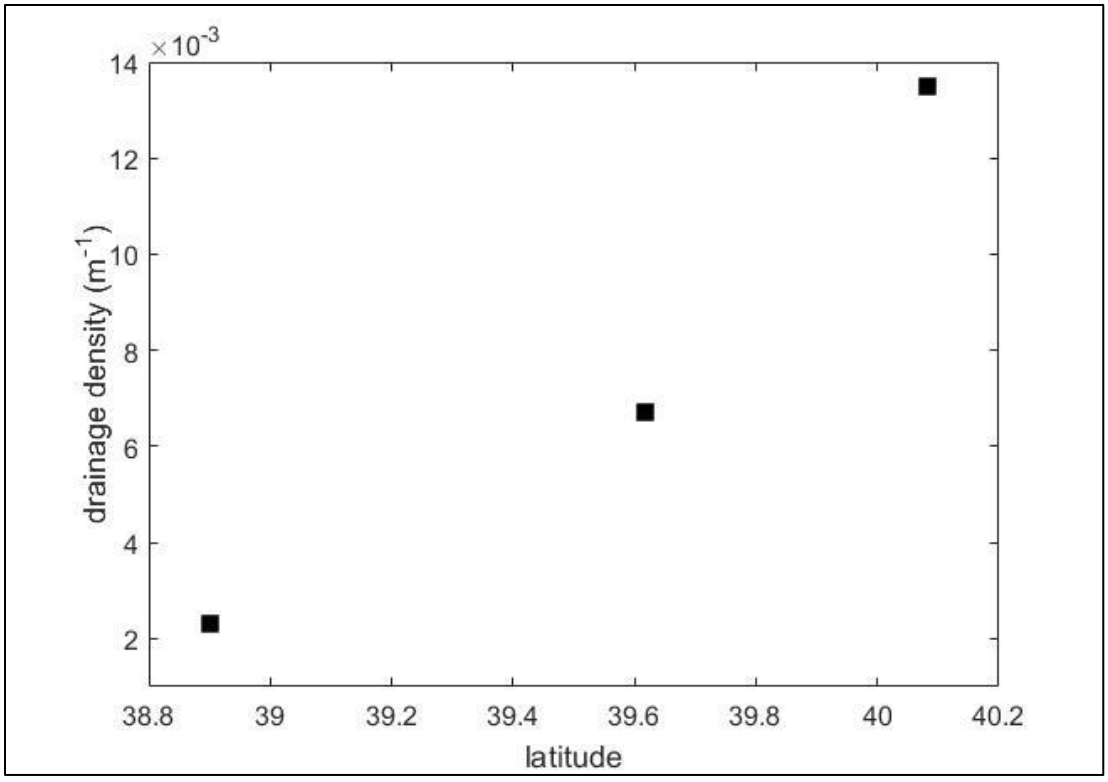

Figure 21: Calculated drainage density as a function of latitude.

We also mapped channel density throughout our main Eel River study area using the focal statistics tool in ArcMap 10.2. We employed a 250m diameter moving circular window to produce local average channel densities (figure 22). This spatial average reveals that drainage density is higher in topographically convergent zones, regardless of whether these zones are occupied by active or relict earthflows. Channel density values within the inter-ridge convergent zones have a general range of ~0.01-0.035m^{-1}, while ridgetops of lower flow accumulation have channel densities of ~0-0.01m^{-1}.

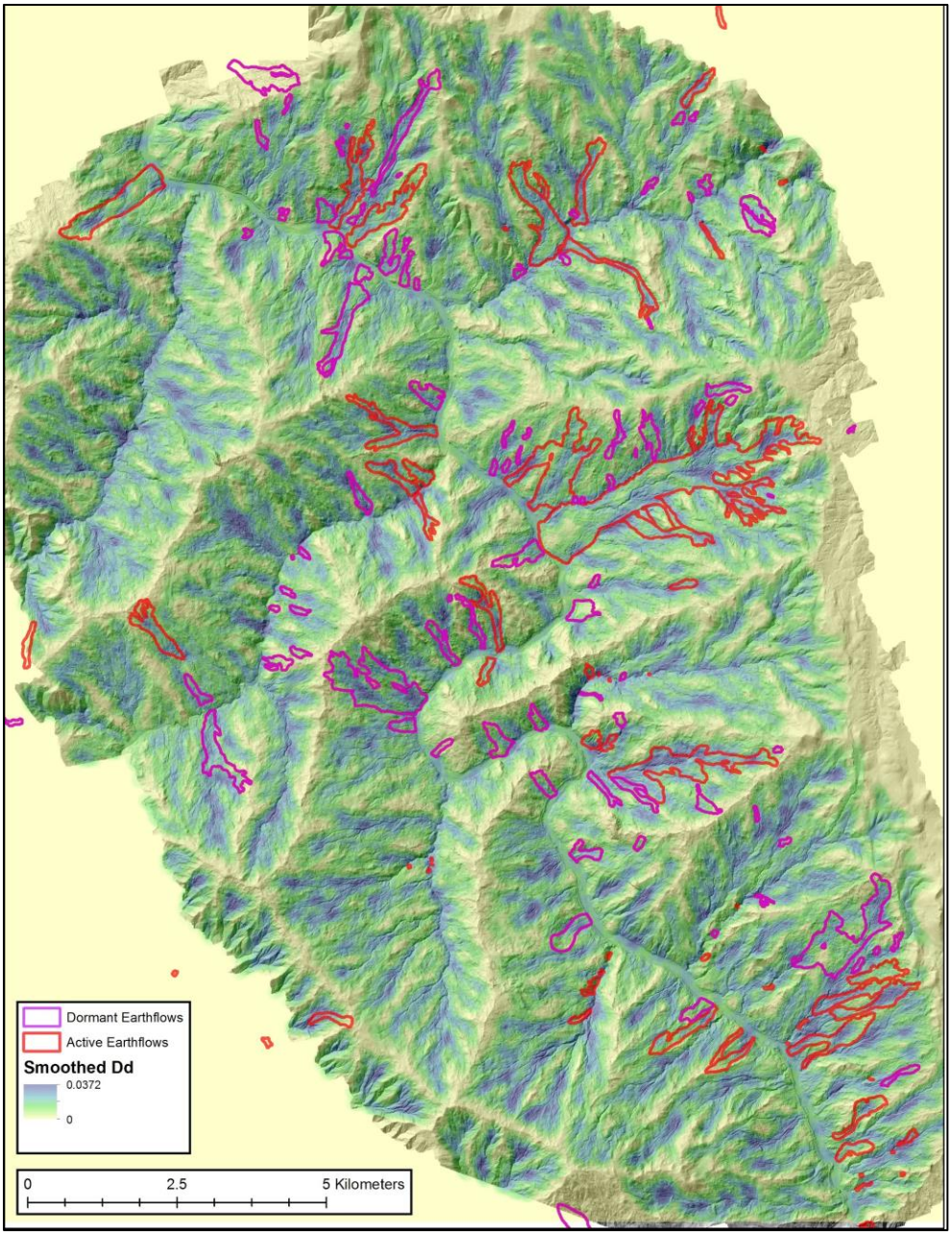

Figure 22: Drainage density in the Central Eel DEM. Calculated with a 250m diameter moving window, using the Focal Statistics tool in ArcGIS 10.2. Gully density is high throughout all topographically convergent zones.

In order to determine if earthflows themselves are the factor instigating gully network formation, we compared channel density values between active earthflows and dormant earthflows mapped by Bennett et al, 2016, and inactive topographic hollows. These hollows were likely active flows at one point, but no longer exhibit the topographic

features (head scarps, lateral levees, inter-ridge fill) typical of active or dormant flows. We analyzed only flows that were at least as large as the smallest inactive zone. Distributions of drainage densities for the three are shown in figure 23. Active flows (n=33) have the highest mean drainage density of 0.0276m^{-1}, with a standard error of 0.0017. Dormant flows (n=40) have a remarkably similar mean drainage density of 0.0274m^{-1}, with a standard error of 0.0015. Inactive catchments (n=18) have a lower mean drainage density, 0.0192m^{-1}, with a standard error of 0.0010. The difference in means between active/dormant flows and inactive zones is statistically significant, with a p-value of 0.0033.

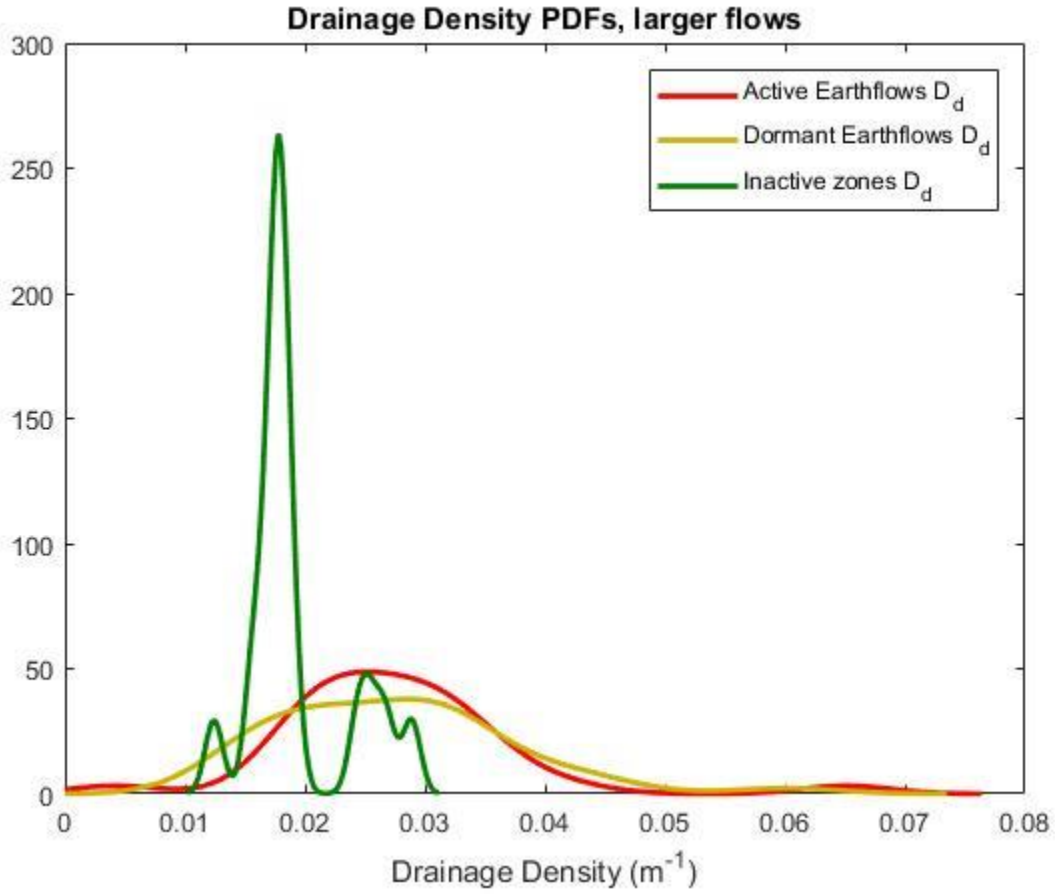

Figure 23: Probability density functions of drainage density for active, dormant, and inactive zones.

Channel Curvature Variance Results

In order to quantify differences in channel undulations in different stages of flow activity, we compute curvature and the standard deviation of curvature across different scales for active, dormant, and inactive trunk streams throughout our Central Eel DEM. This computation was performed 60 times on each channel with a local radius of curvature between 5m and 300m, increasing by 5m each iteration. Since local curvature is computed for each point on a stream profile, each stream will have a distribution of curvature values, the size of which is equal to the number of points in the profile. We compute the standard deviation of curvature (a measure of how much a profile undulates) for each stream, and take the mean of all the standard deviations across all streams. The mean standard deviation of local curvature varies between active, dormant, and inactive zones, dependent upon the radius of the curvature calculation. Curvature variance for channels on active and dormant earthflows largely track each other across all radii, but trunk streams in inactive zones diverge significantly for lower radii. In inactive channels over small radii, variance is larger, meaning channels are undulating more over small length scales. For intermediate radii in inactive channels, variance is lower (figure 24). A statistical ANOVA test confirms a significant difference in curvature variances between the three (figure 25).

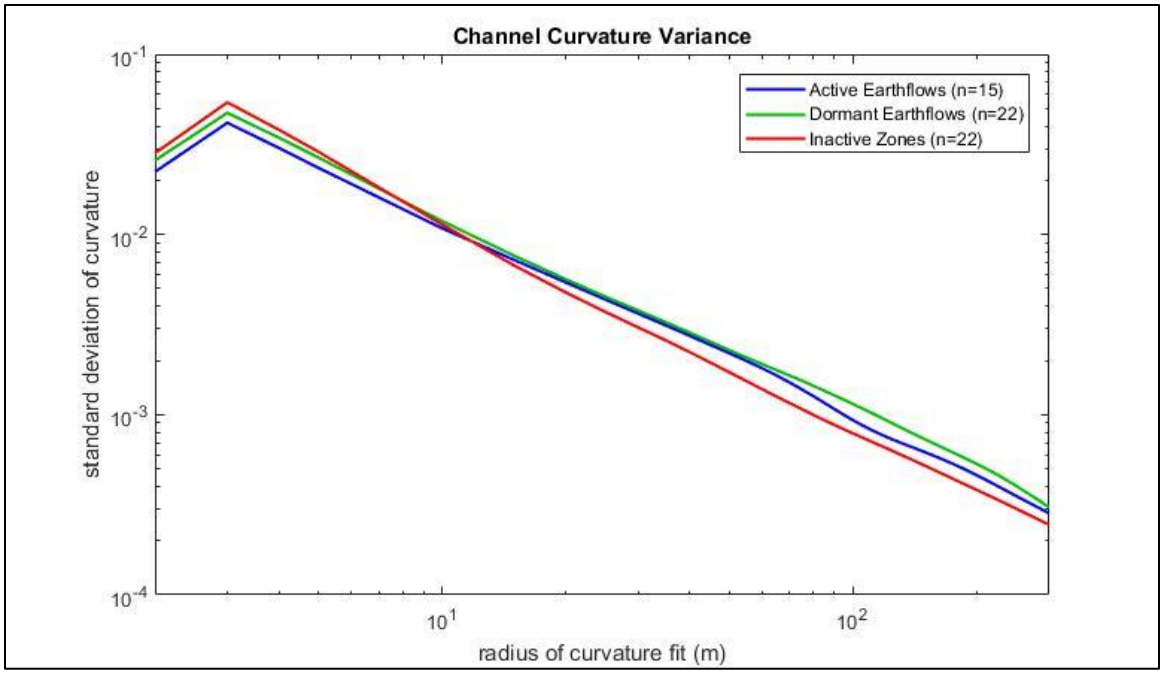

Figure 24: Mean standard deviation of local curvature as a function of the radius of calculation (m).

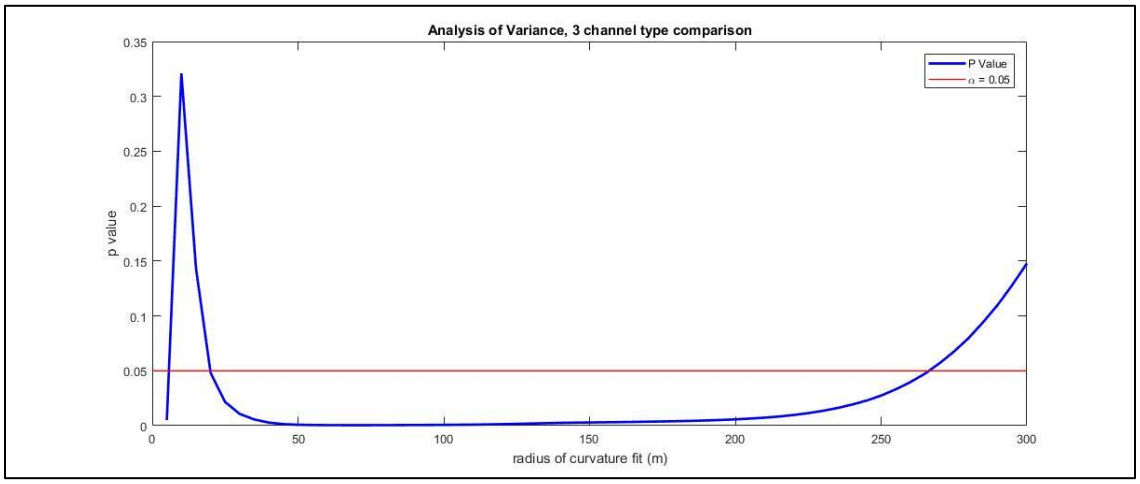

Figure 25: Statistical analysis of variance (ANOVA) of the curvature variance between the three channel types. P values below the alpha value of 0.05 denote radii with statistically significant differences in curvature variance.

Discussion

We find a marked increase in drainage density with tectonic uplift between our three DEMs in the Central Franciscan mélange. This implies that A) low-order ephemeral gullies, are important agents in exporting sediment to higher order channels to balance uplift, or that B) Earthflows themselves are effective in promoting gully formation and network expansion.

Earthflows classified as "dormant" and "active" show no significant difference in Dd values, while inter-ridge convergent zones have lower Dd values. The similarity in Dd values between active and dormant flows is not surprising. Dormant and active flows were classified based on aerial imagery dating to 1940 (Bennett et al, 2016). As such, dormant flows likely have been active in the recent past, as recently as 1940. Since dormant earthflows display little morphological change from active earthflows, other than attenuation of small-scale surface roughness, it would be unreasonable to presume significant change in drainage density for their associated channel networks. The lower drainage density values of inactive zones might be explained by the migration and eventual merging of lateral levee-pinned channels on each side of the earthflow. As these channels progressively incise and export earthflow sediment, they would slowly migrate towards the true thalweg of the valley, previously occupied by the earthflow body. The joining of two lateral channels into one would effectively halve the channel length in this section, lowering overall drainage density and promoting the formation of a more organized, hierarchical drainage network in the new v-shaped valley.

Field and LIDAR observations provide indications as to the evolution of a channel network after its associated earthflow stops moving. Networks on active flows are characterized by immature channels truncated by alluvial fans, and pervasive lateral bank failure during high runoff events. Dormant flows, while displaying many similar features to active flows, do not have networks with alluvial fans, and channel banks are generally smoother and exhibit infrequent mass failure, as they are not being constantly destabilized by channel migration that results from slide movement. Finally, watersheds

that are not occupied by earthflow features display more mature, classically organized dendritic networks, with armored beds and incised channels.

These qualitative observations are supported by our calculations on the variance in curvature between channel types. Variance in curvature at a large radius of fit does not differ greatly between active, dormant, and inactive zones, since this radius is much larger (250-300m) than the scale at which earthflow undulations are relevant. At smaller scales (2-20m), channels in inactive zones display a significantly higher variance in curvature. This may reflect the presence of large metamorphics that have accumulated in the channel after progressive incision, which dictate large fluctuation in curvature as they compose the channel bed. In intermediate scales, inactive channels exhibit a lower variance in curvature, which likely indicates incision through an earthflow's undulations, which previously were the dominant control on the channel long profile. Based on these observations, we suggest that channel networks paired with earthflows follow a general course of evolution:

Earthflows, while active, dominate the form and sediment supply to low order channels on their surface. Channels navigate hummocky topography dictated by the earthflow basal slip surface (Coe et al. 2009), incising in steeper sections, and depositing sediment in lower-slope areas. This creates a poorly integrated channel network, with longitudinal profiles undulating above and below a constant slope. After the earthflow stops moving, streams are given the opportunity to incise without interference of advective downslope movement. Gully headcuts from steeper, incised channel sections can propagate into low-slope depositional fans, thereby connecting previously disrupted channels. This allows coarse sediment to bypass low-slope areas in greater quantities, and channels can become decoupled from topography created by earthflow shear layer geometry. After channels dissect low-slope depositional areas, they then incise further into the stationary earthflow body, organizing the network into a dendritic pattern. Channels previously pinned on the outside of earthflow levees coalesce into a single trunk stream, and form a classic v-shaped valley, dominated by fluvial incision.

It’s possible that in this phase, incision and morphologic change is limited, as channels accumulate the large Franciscan metamorphic clasts, previously carried within the earthflow body. These clasts are too large for fluvial transport, leading to armoring of the channel bed, shielding smaller clasts from transport, and thereby limiting available incisional tools. This incision limitation could then serve as an initial condition necessary to reactivate earthflow movement, as the channels cannot incise to adjust to continuing uplift (figure 26, below). This interplay between earthflow-dominant and fluvial-dominant behavior may be a valuable tool in future predictions of long-term sediment transport and landscape evolution behaviors in this landscape.

A)

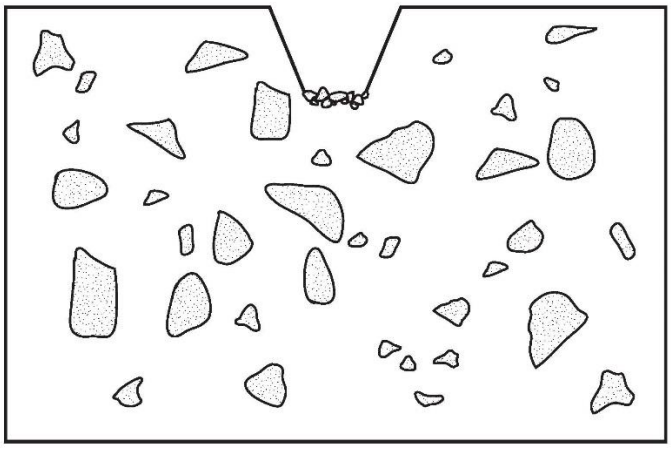

B)

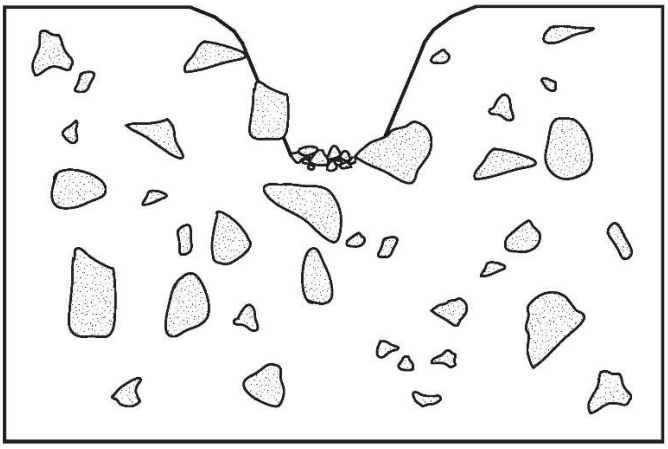

C)

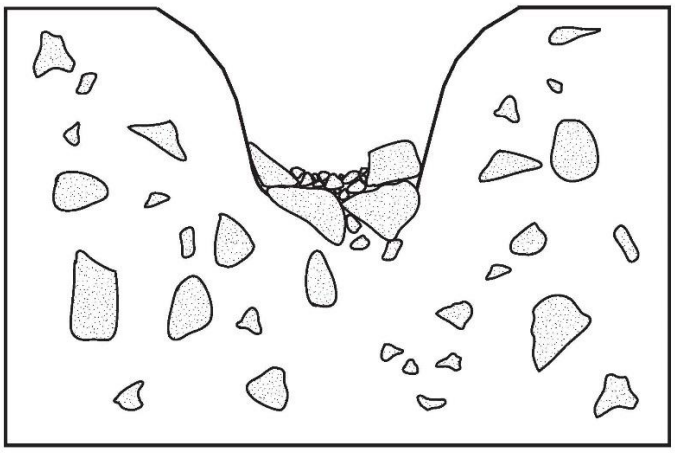

Figure 26: Evolution model of channels coupled to active earthflows. A) Earthflow advects mass through channelized area, inhibiting incision. B) The earthflow ceases movement, and the channel incises downward into the earthflow body. C) The channel accumulates Franciscan megaclasts, armoring the bed and stopping further incision. This leads to reinitiation of earthflow movement via hillslope over steepening.

CHAPTER III

SEDIMENT FLUX AND ALLUVIAL FANS

Background

To estimate the sediment flux of gully networks in our earthflow-dominated study area, we employ the presence of the rather unique low-slope sections in stream networks, which promote formation of alluvial fans as channels traverse them. By calculating the rate of deposition in these fans, we estimate a minimum sediment transport capacity of earthflow-coupled gullies.

We have focused on the channels coupled with one earthflow, called the Kekawaka slide (Mackey & Roering, 2011). The Kekawaka flow displays typical behavior of earthflows in the area. It flows from north to south, with its toe terminating at the banks of Kekawaka Creek, a tributary to the main stem of the Central Fork Eel River. It has an average annual velocity of 0.85m/yr and an annual sediment flux of 2551m^3/yr from translating material directly into Kekawaka Creek (Mackey & Roering, 2011; Bennett et al, 2016). It displays the typical "hourglass" shape of many earthflows in the area, as described by Mackey & Roering (2011) and Kelsey (1978). It features a wider, amphitheater-like headscarp and accumulation area, a thinner and elongate transport zone, and a wider toe, where sediment spreads out as it encounters the lower slope of Kekawaka Creek. In keeping with other earthflows in the area, Kekawaka slide exhibits an irregular and undulatory longitudinal profile (figure 16), which we predict to roughly match that of the basal shear boundary at its base. The geometry of this boundary is likely governed by the distribution of large metamorphic clasts within the Franciscan mélange bedrock (Kim et al, 2004).

The gully network associated with the Kekawaka slide must navigate the same undulatory geometry that determines the surface of the earthflow. As a result, streams incise more deeply into slide areas of greater slope, and deposit fluvial sediment on low slope areas in wide alluvial fans (photos 3 and 4). These fans show signs of fluvial

imbrication, indicating that they are not the results of debris flows. Growth of vegetation on fan margins indicate the extent of the previous rainy season's deposition of fan material. Some of these depressions also form seasonal ponds, in areas where the earthflow is able to impound water as well as sediment. We expect that these fans and ponds are stationary in their location, and that earthflow movement advects mass through them. This opens accommodation space by conveying sediment out of the deposition zone annually. Coe et al (2009) observed similar translating fans and pond deposits on the Slumgullion slide in Southwestern Colorado, and concluded that the locations of fan and pond-forming depressions were determined by basal shear boundary geometry. Notably, we visually observe that these fans are composed primarily of coarse (>1cm) sediment, in higher concentrations than the body of the earthflow from which the sediment is sourced. This implies that some proportion of fine sediment bypasses the fans as suspended load. On Kekawaka slide and other observed earthflows, alluvial fans are concentrated in the upper end of the translational zone, where flow accumulation is lesser, and gullies lack the capacity to incise through low-slope earthflow material faster than the earthflow can advect sediment through.

Since channel banks are highly unstable, normal instrumentation and gauging stations are precluded from use in estimating sediment transport. Without traditional means to measure sediment flux in these channels, we can measure the deposition in low-slope alluvial fans to establish a minimum rate of sediment transport by earthflow-coupled gully networks. In our study, we focus on the gullies and alluvial fans of Kekawaka slide to infer the overall sediment contribution of earthflow-paired channels in this system.

Methods

Calculating gully sediment transport at fan sites

We use deposition in alluvial fans to determine a minimum sediment transport rate for earthflow-coupled gullies. In order to do so, we operate under the assumption that

alluvial fan and pond locations and geometry are determined by the earthflow basal shear boundary, and therefore are static throughout time. In order for alluvial fans to maintain their geometry, the gully sediment flux at the fan head must be greater than or equal to the rate of accommodation space creation by earthflow translation. Thus, we can calculate rate of accommodation space creation as

$$V = wdv$$

where *w* is the width of the fan, parallel to downhill earthflow movement, *d* is the average depth of the fan, and *v* is the annual velocity of the earthflow. Multiplying these three terms yields the rate at which fan material is advected out of the static zone of deposition, thereby creating space for more sediment deposition. In units of kg per year, the deposition rate (D) is

$$D = V(\rho c * Cprop + \rho f * (1 - Cprop))$$

where *Cprop* is the mass fraction of coarse sediment deposited in fans, ρ_c is the density of coarse sediment, in kg/m^3, and ρ_f is the density of fine material in kg/m^3. As noted above, we inferred that some proportion of fine sediment, carried as suspension, bypasses these alluvial reaches as coarse sediment is preferentially deposited. If the sediment is delivered to channels indiscriminately - that is, the grain size distribution within the earthflow body is the same as is introduced to channels - then we can quantify the amount of fine sediment that bypasses the fans and immediately enters the high order network by examining the difference in the proportion of coarse material (>1cm) between earthflow colluvium and sediment deposited in the alluvial fans. This can be quantified as

$$Fs = \left(\frac{Ef}{Ec} - \frac{1 - Cprop}{Cprop}\right) D$$

where Fs is the mass (kg/yr) of fine sediment that bypasses the fan, Ef is the proportion of earthflow colluvium expressed in the fine fraction, and Ec is the proportion of earthflow colluvium expressed in the coarse fraction. Combining the accommodation space deposition and fine sediment that bypasses the fan would yield a sediment flux of

$$Q = D + Fs$$

Determining alluvial fan dimensions

To determine the planform dimensions of alluvial fans on the surface of Kekawaka slide, we used a Trimble 2008 GeoXH GPS to outline the extent of seasonal alluviation (figure 27 and 28). GPS measurements were taken during the summer of 2016. Unvegetated fan material was interpreted to be deposited during last rainy season, when ephemeral gullies were active and fluvially transporting bedload material. Some areas in fans featured course deposited material, but were also overgrown with large plants, and we determined that these areas were not alluviated or fluvially reworked in the last season, or plants would not have been able to grow. Calculation of fan planform area based on this criteria may be subject to bias, based on the variability of rainfall and sediment transport year to year. However, we expect that the primary controlling factor on depositional space is the geometry of the depression itself, which does not vary. Distal fan areas with finer deposited sediment and some vegetation were also mapped by GPS.

To determine the depths of alluvial fans on Kekawaka, we dug several pits in three of the larger fans. We stopped digging downward when either **a)** material was no longer clast-supported, and was dominated by clay and soil, indicating a transition between the fan deposit and the earthflow body, or **b)** we were unable to keep digging. Overall, we dug 4 pits in one of the uppermost fans on Kekawaka slide, which we label Fan 1, we dug 4 pits in Fan 2 about ¼ of the way down the slide, and finally dug 6 pits in Fan 3, ½ of the way down the slide, which spans most of the slide width. See figures 27 and 28 for fan and sample pit locations. We encountered earthflow soil matrix in most cases within one to two meters, which represents the alluvial fan depths.

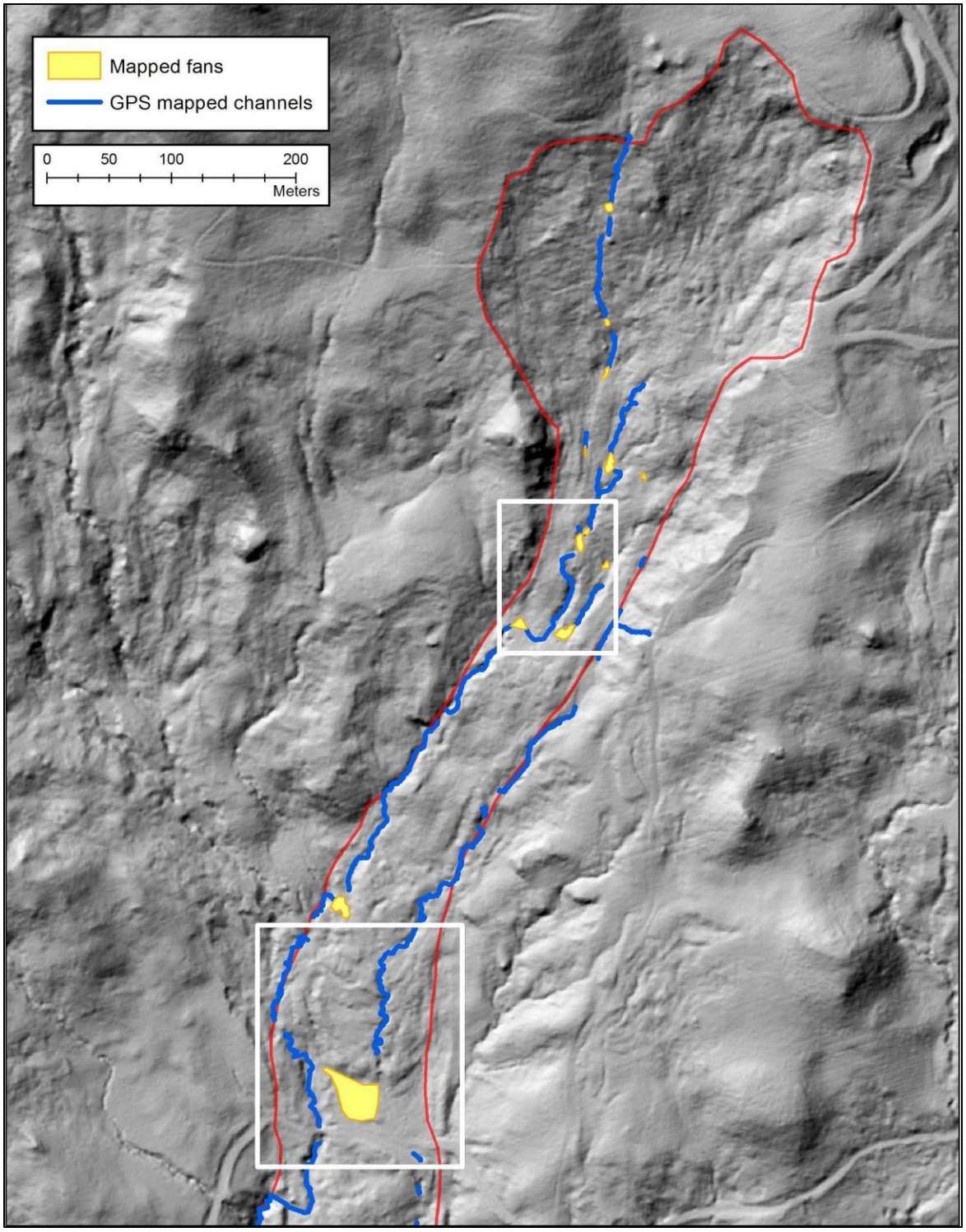

Figure 27: The upper half of Kekawaka slide, with GPS-mapped channels (blue), and GPS-mapped alluvial fans (yellow). The upper white box frames figure 28a (below), containing fans 1 and 2. The lower white box frames figure 28b (below), containing fan 3.

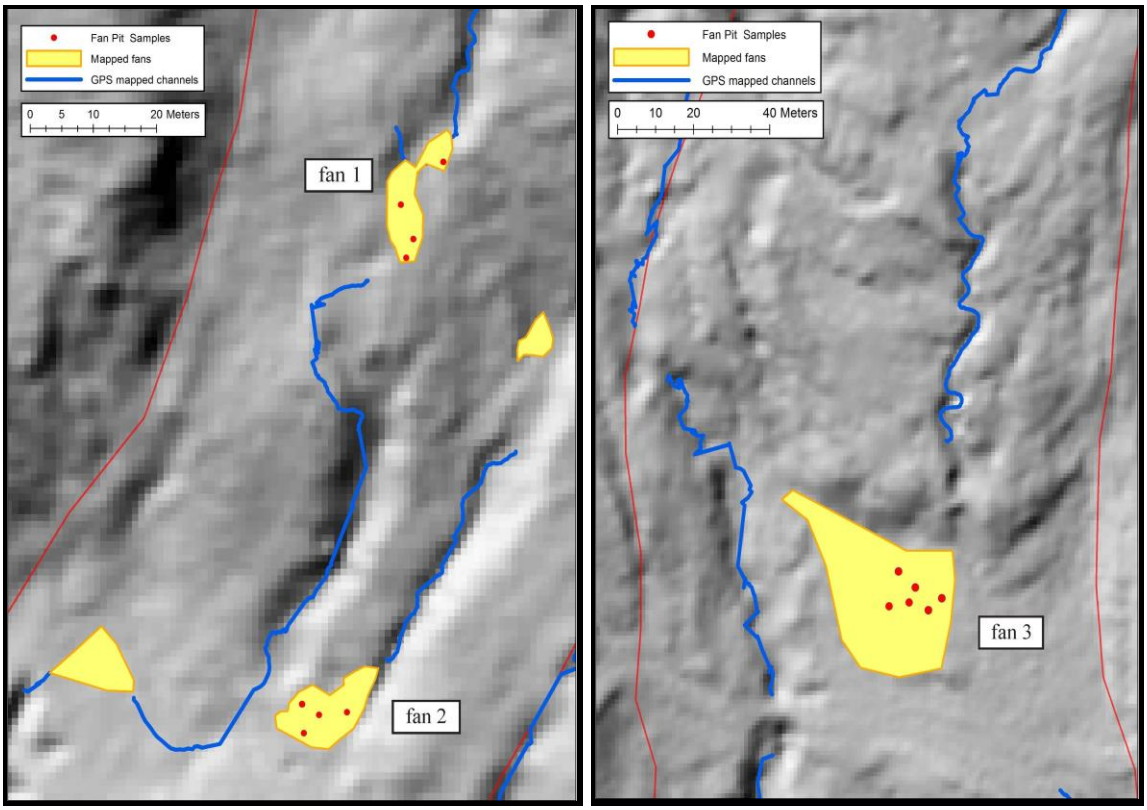

Figure 28: Alluvial fans 1, 2, and 3 on Kekawaka Slide. Red dots denote locations where pits were dug to determine fan depth.

Determining Mass Fractions and Grain Size Distributions of Fans, Channels, and Colluvium

The Franciscan Complex is composed of clasts spanning a full range of grain size, from sand and silt to clasts the size of city blocks. Earthflow movement and fluvial processes are capable of transporting very different ranges of grain sizes. In an attempt to quantify the transport capacity and limitations of gullies, we used several methods to determine grain size distribution differences between channels, fans, and the earthflow matrix.

To determine the grain size distribution of gully channel beds above alluvial fans, we used the pebble count method (Kondolf and Li, 1992). Most channels were not wide enough to walk across and obtain more than ~2 measurements, so counts were acquired

by walking up and down channel sections of relatively consistent slope until a sufficiently large sample size (>100 measurements) was achieved.

After digging pits in alluvial fans to determine depth, we collected sediment samples from the side walls of at least one pit per fan. The smallest sample weighed 0.95kg. Samples were later sorted with a mechanical sieve at 0.36 and 0.8cm widths, and each class from 0-0.36cm, 0.36-0.8cm, and >0.8cm were weighed with a 0.01kg-precision scale. All b-axis measurements of clasts over 0.8cm were also recorded by hand measurement to determine grain size distribution in the coarse fragment.

To determine the fraction of mélange-derived colluvium clasts over 1cm, we took two photos of road cuts into colluvium (photo 6). On these photos, we overlaid a grid of ~1cm width, and for each line intersection, we recorded whether the intersection coincided with a clast with a b-axis larger or smaller than the 1cm grid spacing. Each photo consisted of over 2000 point measurements. To determine volumetric proportion from a planform image, we operate under the assumption that areal proportions are equivalent to volumetric proportions (Medley, 1994), provided there is no preferred orientation of larger clasts within the matrix. With only two photos of colluvium, however, this assumption may lead to significant error (Haneberg, 2004). To convert volumetric proportion to mass proportion, we employed a water displacement test to determine density of coarse sediment (primarily greywacke sandstone) and fine sediment.

Photo 6: Exposed Franciscan colluvium, with overlying grid. Field notebook (height 14cm) for scale.

Results

Alluvial fan depths

For fan 1, pits yielded a mean depth of 56.25cm. Fan 2 had a mean depth of 46.5cm. Fan 3 had a mean depth of 48.5cm.

Fan 1	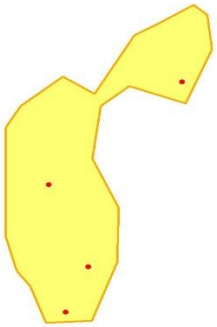	Pit matrix depths (top to bottom) Pit 1: 45cm Pit 2: 65cm Pit 3; 65cm Pit 4: 50cm Course sediment mass component: 0.32
Fan 2	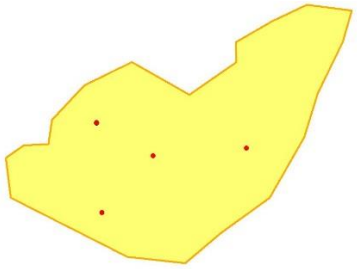	Pit matrix depths (left to right) Pit 1: 21cm Pit 2: 36cm Pit 3: 77cm Pit 4: 55cm Course sediment mass component: 0.29
Fan 3	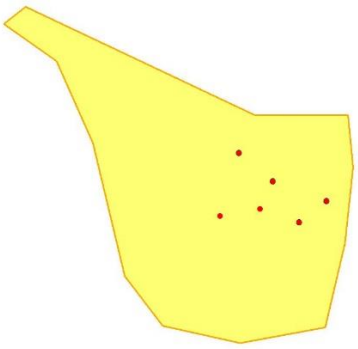	Pit matrix depths (left to right) Pit 1: 25cm Pit 2: 63cm Pit 3: 60cm Pit 4: 82cm Pit 5: 10cm Pit 6: 51cm Course sediment mass component: 0.27

Figure 29: Outlines of fans, 1, 2, and 3, with individual pit depths and course sediment fractions.

Alluvial fan planform dimensions

Perimeters of alluvial fans were walked with GPS, and shapes of fans varied between features, dependent upon local earthflow morphology. For fans 1, 2, 3 on Kekawaka slide, upon which we base our analysis, fan widths were 7m, 10m, and 32m respectively.

Coarse and fine sediment fractions from fans and colluvium

From sorting and weighing pit samples from fans 1, 2, and 3, we measured the mass fractions of coarse grain deposition to be 0.32, 0.29, and 0.27, respectively. From our colluvium photo point counts, we arrived at a planform coarse sediment proportion (Vc) of 0.2516, which would result in a volumetric proportion of the same value, and a volumetric fine proportion of 0.7484 (V_f). We adjust this volumetric proportion to a mass proportion with the following equation:

$$Ec = \frac{Vc * \rho c}{Vc * \rho c + Vf * \rho f}$$

15 water displacement measurements of course sediment yielded a density of 2733kg/m^3 (ρc), and 10 measurements of fine sediment yielded a density of 2170kg/m^3 (ρf). This results in a course sediment mass proportion of 0.2975 in the earthflow colluvium, which is remarkably similar to mass proportions we measure from alluvial fan samples. As a result, we are compelled to dismiss calculation of the fine material that bypasses alluvial fans as suspended load. Minimum annual sediment flux for channels entering our three alluvial fans on Kekawaka slide then simply equals accommodation space created annually by earthflow movement (Equation 1). This results in the following sediment fluxes:

Fan 1 flux = 7866 kg/yr or 3.35m^3/yr
Fan 2 flux = 9222.25 kg/yr or 3.95 m^3/yr
Fan 3 flux = 30,632 kg/yr or 13.19 m^3/yr

Fans 1 and 2 lie in a different sub-drainage than fan 3 on Kekawaka slide, so we can combine the highest flux value between fans 1 and 2 with that of fan 3 to obtain a minimum fluvial flux of 39,854kg/yr or 17.14m^3/yr. Mackey and Roering (2011) calculated the annual sediment flux for the Kekawaka slide to be 2551m^3/yr, based on measurements of slide width, depth and velocity. Our calculation of minimum fluvial sediment transport is therefore only 0.7% of sediment transport by earthflow sliding

Discussion

Though our calculated fluvial proportion of overall earthflow sediment flux is negligibly low, it is worth noting that our estimation is a minimum value, calculated only from sediment that was deposited on the earthflow's upper portion, where channels do not have enough flow accumulation to incise through hummocks, and have not been pushed to the lateral boundaries of the earthflow. In reality, it's likely that fluvial sediment transport exceeds our calculated rate by a large margin. In the field, we see definitive evidence of sediment, both fine and coarse, that bypasses fans during large runoff events (photos 7 and 8). Additionally, sediment flux, by virtue of being tied to the locations of the alluvial fans, is calculated at relatively low drainage areas - all three fans lie within the upper half of the earthflow, and the maximum flow accumulation between these three fans is 133,700m^2, compared to 1,562,000m^2 at the confluence of the main gully from Kekawaka slide with Kekawaka Creek. We expect that fluvial sediment entrainment and transport will be greater downstream, where higher flow accumulation provides greater shear stresses to transport sediment being introduced to the fluvial network via earthflow movement. Indeed, Kelsey (1978) estimated that gully networks in this region contribute a roughly equal amount of sediment to the main channel as earthflows.


Photos 7 and 8: Evidence of course sediment bypassing fans. Both photos are taken at the site of fan 2. The person in the left photo is standing on a deposit which spilled over the primary fan, in the background. The right photo was taken from fan 2, looking down on the incipient channel behind the person in the left photo.

The similarity between the measured mass proportion in alluvial fans and in Franciscan Complex colluvium is an unexpected result, as we expected to find an abundance of coarse material in the fans relative to the colluvium introduced to channels. As it stands, the results of course mass fraction do not match our visual observations from the field, where we saw that fans were supported by clasts at depth, while channel banks and earthflow colluvium were not. The discrepancy between our observations and measurements can be due to a variety of factors:

1. Our sampling of alluvial sediment was flawed, and favored the collection of fine grains over coarse clasts.
2. We did not sufficiently sample fans to capture an accurate grain size distribution of alluvial fans.

3. Channels uphill of alluvial fans effectively sorted sediment such that larger clasts, which may make up the majority of mass in the coarse grain fraction, are never deposited in the fans.
4. In the sieving process, coarse grains broke down, and were recorded as fine material.
5. We did not have a large enough sample size in measuring colluvial coarse grain volume. A more accurate count would be possible with more photos.
6. We may have mistaken coherent soil peds within our photos to be course metamorphics, thereby overestimating course volumetric block proportion.

As a result, we expect that our flux calculations, while already being minimum estimates of fluvial flux, drastically underestimate the true flux of channels on the Kekawaka slide by virtue of ignoring the transport of sediment past that which is deposited in alluvial fans. In several fans, we not only visually observe a saturation of course grains in fans (due to fine sediment bypassing as suspension), but also evidence of course sediment grains that bypass fans as bedload.

To more accurately estimate fluvial sediment flux in this area, different methods could be used to directly measure sediment transport. These may include weirs at channel outlets, suspended sediment samples during runoff events, or repeat remote sensing to determine changes in alluvial fan and channel morphology. In particular, study of differences in fluvial sediment flux between active, dormant, and incised slides would be useful in informing the relative importance of channels in sedimentation within the Eel River, and areas with high levels of mass wasting in general.

Conclusion

The Central belt of the Franciscan Complex contains a significant gradient in tectonic uplift, due to its parallel orientation to the Mendocino Triple Junction Crustal Conveyor. Previous research (Bennett et al, 2016a, Mackey and Roering, 2015) has demonstrated the importance of mass wasting in contributing to denudation in pace with this uplift. We find that mas wasting also exerts a strong control on the fluvial networks within the Franciscan Complex. We find a consistent increase in drainage density with increased earthflow activity, both between areas of differing uplift and mass wasting, and between low-order valleys of differing earthflow activity within the same geographic area. In the long profiles of channels across the study area, we find differences in curvature relating to the morphology of earthflows, and the composition of the material through which channels must incise. From this, we propose a feedback model between channels and earthflows that may explain how a hillslope cycles between primary mechanisms of erosion - mass wasting and fluvial incision.

We also investigate the sediment transport capacity of gullies on the surface of large, slow-moving landslides. We find a relatively low sediment flux contribution from channels coupled to earthflows. This is due to the fact that we estimate flux on upper reaches of the slides, where flow accumulation is less and therefore transport capacity is smaller. This low estimation is also likely due to errors in measurement. A more precise fluvial sediment contribution in this area is open to further inquiry.

Another important conclusion from this work is that in this landscape, the Central Franciscan bedrock exerts a very strong influence on both fluvial and hillslope erosive processes. The weak, sheared argillite matrix and fractally distributed hard metamorphics of the Central Franciscan Complex conspire to create long, low-angle hillslopes prone to failure, with internal structure that creates irregular undulations in both earthflows and the channels that dissect them.

REFERENCES CITED

1. Balco, Greg, et al. "Erosional response to northward-propagating crustal thickening in the coastal ranges of the US Pacific Northwest." *American Journal of Science* 313.8 (2013): 790-806.

2. Bennett, Georgina L., et al. "Landslides, threshold slopes, and the survival of relict terrain in the wake of the Mendocino Triple Junction." *Geology* 44.5 (2016): 363-366.

3. Brown, William M., and John R. Ritter. "Sediment transport and turbidity in the Eel River basin, California." (1971).

4. Burkard, M. B., and R. A. Kostaschuk. "Initiation and evolution of gullies along the shoreline of Lake Huron." *Geomorphology* 14.3 (1995): 211-219.

5. Coe, Jeffrey A., et al. "Basal-topographic control of stationary ponds on a continuously moving landslide." *Earth Surface Processes and Landforms*34.2 (2009): 264-279.

6. DeRose, R. C., et al. "Gully erosion in Mangatu Forest, New Zealand, estimated from digital elevation models." *Earth Surface Processes and Landforms* 23.11 (1998): 1045-1053.

7. Ferrier, Ken L., James W. Kirchner, and Robert C. Finkel. "Erosion rates over millennial and decadal timescales at Caspar Creek and Redwood Creek, northern California Coast Ranges." *Earth Surface Processes and Landforms*30.8 (2005): 1025-1038.

8. Furlong, Kevin P., and Rob Govers. "Ephemeral crustal thickening at a triple junction: The Mendocino crustal conveyor." *Geology* 27.2 (1999): 127-130.

9. Golly, Antonius, et al. "Controls and feedbacks in the coupling of mountain channels and hillslopes." *Geology* 45.4 (2017): 307-310.

10. Gordon, Lee M., et al. "Modeling long-term soil losses on agricultural fields due to ephemeral gully erosion." *Journal of soil and water conservation* 63.4 (2008): 173-181.

11. Handwerger, Alexander L., Joshua J. Roering, and David A. Schmidt. "Controls on the seasonal deformation of slow-moving landslides." *Earth and Planetary Science Letters* 377 (2013): 239-247.

12. Handwerger, Alexander L., et al. "Kinematics of earthflows in the Northern California Coast Ranges using satellite interferometry." *Geomorphology* 246 (2015): 321-333.

13. Haneberg, William C. "Simulation of 3D block populations to characterize outcrop sampling bias in bimrocks." *Felsbau Rock and Soil Engineering Journal for Eng. Geology, Geomechanics and Tunneling* 22.5 (2004).

14. Kelsey, Harvey M. "Earthflows in Franciscan mélange, Van Duzen River basin, California." *Geology* 6.6 (1978): 361-364.

15. Kim, Carl, Charles Smell, and Edmund Medley. "Shear strength of Franciscan Complex mélange as calculated from back-analysis of a landslide." (2004).

16. Knapen, Anke, et al. "Resistance of soils to concentrated flow erosion: A review." *Earth-Science Reviews* 80.1 (2007): 75-109.

17. Kondolf, G. Mathias, and S. Li. "The pebble count technique for quantifying surface bed material size in instream flow studies." *Rivers* 3.2 (1992): 80-87.

18. Korup, Oliver. "Geomorphic imprint of landslides on alpine river systems, southwest New Zealand." *Earth Surface Processes and Landforms* 30.7 (2005): 783-800.

19. Lock, Jane, et al. "Late Neogene and Quaternary landscape evolution of the northern California Coast Ranges: Evidence for Mendocino triple junction tectonics." *Geological Society of America Bulletin* 118.9-10 (2006): 1232-1246.

20. Mackey, B. H., J. J. Roering, and J. A. McKean. "Long-term kinematics and sediment flux of an active earthflow, Eel River, California." *Geology* 37.9 (2009): 803-806.

21. Mackey, Benjamin H., and Joshua J. Roering. "Sediment yield, spatial characteristics, and the long-term evolution of active earthflows determined from airborne LiDAR and historical aerial photographs, Eel River, California." *Geological Society of America Bulletin* 123.7-8 (2011): 1560-1576.

22. Marden, Michael, et al. "Pre-and post-reforestation gully development in Mangatu Forest, East Coast, North Island, New Zealand." *River Research and Applications* 21.7 (2005): 757-771.

23. McLaughlin, Robert J., et al. "Geology of the Cape Mendocino, Eureka, Garberville, and southwestern part of the Hayfork 30× 60 minute quadrangles and adjacent offshore area, northern California." *US Geological Survey Miscellaneous Field Studies Map MF-2336* 1.100 (2000): 000.

24. Medley, Edmund, and Richard E. Goodman. "Estimating the block volumetric proportions of melanges and similar block-in-matrix rocks (bimrocks)." *1st North American Rock Mechanics Symposium*. American Rock Mechanics Association, 1994.

25. Moody, John A., and David A. Kinner. "Spatial structures of stream and hillslope drainage networks following gully erosion after wildfire." *Earth Surface Processes and Landforms* 31.3 (2006): 319-337.

26. Nyssen, Jan, et al. "Removal of rock fragments and its effect on soil loss and crop yield, Tigray, Ethiopia." *Soil Use and Management* 17.3 (2001): 179-187.

27. Oguchi, Takashi. "Drainage density and relative relief in humid steep mountains with frequent slope failure." *Earth Surface Processes and Landforms* 22.2 (1997): 107-120.

28. Parkner, Thomas, et al. "Development and controlling factors of gullies and gully complexes, East Coast, New Zealand." *Earth Surface Processes and Landforms* 31.2 (2006): 187-199.

29. Passalacqua, Paola, Paolo Tarolli, and Efi Foufoula-Georgiou. "Testing space-scale methodologies for automatic geomorphic feature extraction from lidar in a complex mountainous landscape." *Water resources research* 46.11 (2010).

30. Poesen, Jean, et al. "Gully erosion and environmental change: importance and research needs." *Catena* 50.2 (2003): 91-133.

31. Rengers, Francis K., and G. E. Tucker. "Analysis and modeling of gully headcut dynamics, North American high plains." *Journal of Geophysical Research: Earth Surface* 119.5 (2014): 983-1003.

32. Roering, Joshua J., et al. "Using DInSAR, airborne LiDAR, and archival air photos to quantify landsliding and sediment transport." *Geophysical Research Letters* 36.19 (2009).

33. Roering, Joshua J., et al. "Beyond the angle of repose: A review and synthesis of landslide processes in response to rapid uplift, Eel River, Northern California." *Geomorphology* 236 (2015): 109-131.

34. Sangireddy, Harish, et al. "GeoNet: An open source software for the automatic and objective extraction of channel heads, channel network, and channel morphology from high resolution topography data." *Environmental Modelling & Software* 83 (2016): 58-73.

35. Santangelo, Michele, et al. "Interplay between mass movement and fluvial network organization: An example from southern Apennines, Italy." *Geomorphology* 188 (2013): 54-67.

36. Sidorchuk, A. Yu, and V. N. Golosov. "Erosion and sedimentation on the Russian Plain, II: the history of erosion and sedimentation during the period of intensive agriculture." *Hydrological Processes* 17.16 (2003): 3347-3358.

37. Stankoviansky, Miloš. "Historical evolution of permanent gullies in the Myjava Hill Land, Slovakia." *Catena* 51.3 (2003): 223-239.

38. Sutherland, Diane G., et al. "Evolution of a landslide-induced sediment wave in the Navarro River, California." *Geological Society of America Bulletin* 114.8 (2002): 1036-1048.

39. Swanson, F. J., R. L. Graham, and G. E. Grant. "Some effects of slope movements on river channels." *International Symposium on Erosion, Debris Flow and Disaster Prevention. Tsukuba. Japan*. 1985.

40. Valcárcel, M., et al. "Ephemeral gully erosion in northwestern Spain." *Catena*50.2 (2003): 199-216.

41. Vandaele, Karel, and Jean Poesen. "Spatial and temporal patterns of soil erosion rates in an agricultural catchment, central Belgium." *Catena* 25.1 (1995): 213-226.

42. Wheatcroft, R. A., and C. K. Sommerfield. "River sediment flux and shelf sediment accumulation rates on the Pacific Northwest margin." *Continental Shelf Research* 25.3 (2005): 311-332.

43. Willenbring, Jane K., et al. "What does a mean mean? The temporal evolution of detrital cosmogenic denudation rates in a transient landscape." *Geology* 41.12 (2013): 1215-1218.

44. Wondzell, Steven M., and John G. King. "Postfire erosional processes in the Pacific Northwest and Rocky Mountain regions." *Forest Ecology and Management* 178.1 (2003): 75-87.

45. Zhang, Yongguang, et al. "Characteristics and factors controlling the development of ephemeral gullies in cultivated catchments of black soil region, Northeast China." *Soil and Tillage Research* 96.1 (2007): 28-41.